THE CONTINUED STUDY OF SPOUTED BED GASIFICATION OF WESTERN CANADIAN COALS

Final Report
1983-1984

by

A.P. Watkinson, Principal Investigator
G. Cheng, Research Engineer
S. Low, Junior Research Engineer
Department of Chemical Engineering
The University of British Columbia

Work on this project was conducted under the auspices of the Canada Centre for Mineral and Energy Technology-Energy Mines and Resources, Canada.

DSS File No. 12ST.23440-3-9082
DSS Contract Serial No. OST83-00095
CANMET Project No. 23
CANMET Scientific Authority: C.B. Prakash
D. Fung

July 1984

This report should be cited as Contract Report No. OST83-00095

77 pp

DEC 10 1984

MICROMEDIA

TABLE OF CONTENTS

	Page
List of Figures	(i)-(iii)
List of Tables	(iv)
Summary	(v)
1. Introduction	1
2. Modes of Operation	2
3. Char Bed Runs with Non-Caking Coals	2-10
4. Char Bed Runs with Caking Coal	11
5. Agglomerating Ash Runs	14-21
6. Sulphur Balances in Gasification	22-23
7. Catalytic Gasification Runs	24-27
8. In-Bed Gas Composition and Temperature Profiles	28-39
9. Mathematical Model of Gasification in Spouted Bed	40-49
10. Conclusions and Further Work	55-56
References	56
Nomenclature	52

Appendix A Experimental Data
B Pilot Plant Modification
C Work Statement 1983-1984

LIST OF FIGURES

		Page
Fig. 1	Schematic of Pilot Plant	2
Fig. 2a	Effect of Forestburg Coal Feed Rate (M.A.F. basis) on Gas Heating Value at Constant Air Rate	6
Fig. 2b	Comparison of Char Bed Results with Correlation of 1979-82 Inert Bed Data	6
Fig. 3a	Effect of Oxygen/Coal Ratio on Overall Carbon Conversion (Forestburg Coal-Air Gasification)	7
Fig. 3b	Effect of Oxygen/Coal Ratio on Gross Heating Value of Gas (Forestburg Coal-Air Gasification)	7
Fig. 4	Comparison of Efficiency Function for Char Bed Runs with Inert Bed Run Equation from 1979-1982 Results for Forestburg Coal.	9
Fig. 5	Effect of Average Bed Temperature on Gas Heating Value for Oxygen Gasification of Forestburg Coal	9
Fig. 6	Effect of Steam/Oxygen Mass Ratio in the Blast on the H_2/CO Molar Ratio in the Product Gas	10
Fig. 7	Effect of Coal Feed Rate on Gas Heating Value for Oxygen Gasification of Balmer Coal.	10
Fig. 8	Correlation of Balmer Results for Oxygen Gasification	12
Fig. 9	Carbon Conversion versus Average Bed Temperature	12
Fig. 10	Gas Heating Value (a) and Efficiency Factor (b) versus Average Bed Temperature	13
Fig. 11	Effect of Steam/Oxygen Mass Ratio in the Blast on Hydrogen/Carbon Monoxide Molar Ratio in Product Gas.	13
Fig. 12a	Sketch of 8-Port Oxygen Inlet for Agglomeration	15
Fig. 12b	Air Line Modification to 8-Port Oxygen Inlet	15
Fig. 12c	Deposits on Oxygen Ports (Run 97b)	15
Fig. 13a	Single Oxygen Inlet Port for Run 97c	17
Fig. 13b	Photograph of Materials of Type I, II and III (Run 97c)	17

LIST OF FIGURES

cont'd		Page
Fig. 13c	Location of Materials of Type I to III (Run 97c)	17
Fig. 13d	Location of Agglomerates (Run 98)	18
Fig. 13e	New Piping Arrangement for Steam	18
Fig. 13f	Sketch of Agglomerates (Run 99)	18
Fig. 14	Ash Agglomerates Produced from Balmer Coal	21
Fig. 15	Sampling Line for Sulphur Determination	23
Fig. 16	Gas Sampling Probe for In-bed Samples	29
Fig. 17	Schematic Flow Diagram for the Gas Sampling Line	29
Fig. 18	Locations of Sampling Points in the Bed	30
Fig. 19a b,c	Axial Gas Composition Profiles along Positions A, B, C for Forestburg Coal-Air System (Run 93)	31
Fig. 20	Effect of Char Recycling on Composition Profiles for Forestburg Coal-Air System	33
Fig. 21	Effect of Total Bed Height on Composition Profiles for Forestburg Coal-Air System	34
Fig. 22a b,c	Axial Gas Composition Profiles for Forestburg Coal-Oxygen System Along Positions A, B, C (Run 96)	35
Fig. 23	Axial Gas Composition Profiles for Balmer Coal-Oxygen System (Run 103)	36
Fig. 24	Axial Temperature Profiles for Forestburg Coal-Air System (Run 93)	38
Fig. 25	Axial Temperature Profiles for Forestburg Coal-Oxygen System (Run 94)	38
Fig. 26a	Configuration for One-Dimensional Model	41
Fig. 26b	Streamtube Flow in the Annulus	46
Fig. 27	Axial Gas Composition Profile in the Annulus Predicted using One-Dimensional Model	50
Fig. 28	Comparison of Axial H_2 and CO profiles along the Centre of the Annulus	50

LIST OF FIGURES

cont'd		Page
Fig. 29	Axial Gas Composition Profile Predicted for the Spout	51
Fig. 30	Radial Gas Composition Profiles at the Top of the Bed Predicted Using the Streamtube Model	51
Fig. 31	Comparison between Experimental and Predicted Axial Profiles	52

LIST OF TABLES

Table		Page
1	Outline of Operating Modes 1983-4	4
2	Properties of Coal	4
3	Ash Agglomeration Run Particle Size and Composition	19
4	Average Sulphur Contents in Gas Streams	23
5	Potassium Carbonate Content of Treated Coals	27
6	Reactions Assumed in Char Gasification Model	41
7	Kinetic Parameters Used in Gasification Modelling	42
8	Hydrodynamic Parameters for the Model	43
A-1	Run Conditions and Results (All Runs 1983-4)	
A-2	Forestburg Runs - Summary of Results	
A-3	Balmer Runs - Summary of Results	
A-4	Ash Agglomeration Runs - Summary of Results	
A-5	Particle Size and Size Distributions of Coal, Cyclone Products and Knock-Out Drum Dust	

SUMMARY

This report describes work done during 1983-4 on the development of the spouted bed gsifier. Experiments were carried out with air and oxygen gasification of Forestburg and Balmer coals in beds of char. Conditions are demonstrated for running the gasifier in the agglomerating ash mode. Some preliminary tests were run with catalytic gasification of Balmer coal using K_2CO_3 as catalyst. Sulphur levels in the gas for catalytic and non-catalytic gasification are compared. In-bed measured gas concentration and temperature profiles highlight the major differences in oxygen and air gasification and define the combustion region in the spouted bed. A kinetic model of the gasifier, which predicts axial and radial gas composition profiles in the bed given values for the rate constants, flow conditions and geometry, is presented.

1. Introduction

This report describes work done during 1983-1984 on DSS Contract Serial No. OST83-00095. The primary purposes of this continued study of coal gasification in a spouted bed is to develop a simple flexible coal gasification system and to test it on a variety of Western Canadian Coals. The specific objectives for the 1983-1984 period were:

1. Assess gasifier stability when operating with char beds (as opposed to inert beds) of caking and non-caking coals.

2. Evaluate the feasibility of char bed operation in the agglomerating ash mode, as well as the dry-ash mode.

3. Operate the gasifier on a wider size range of coal.

4. Assess sulphurous and particulate species in the raw gas.

5. Carry out preliminary tests on the use of a catalyst to promote gasification of less-reactive bituminous coals.

6. Continue measurements of in-bed gas composition and temperature profiles for the purpose of developing a mathematical model of the gasifier.

These objectives were to be met by carrying out the research in a number of specific tasks. Appendix C lists the tasks in detail, and the following report will discuss the progress towards achieving the above objectives.

Figure 1 shows the existing pilot plant schematic. Details of construction are given in earlier reports (1-4). A series of pilot plant modifications were made during the course of the contract to achieve the stated objectives. These items are described in Appendix B, except for the evolutionary changes at the reactor inlet which were made to successfully achieve ash agglomeration. These latter changes are described in Section 5 below, which covers the ash-agglomeration tests.

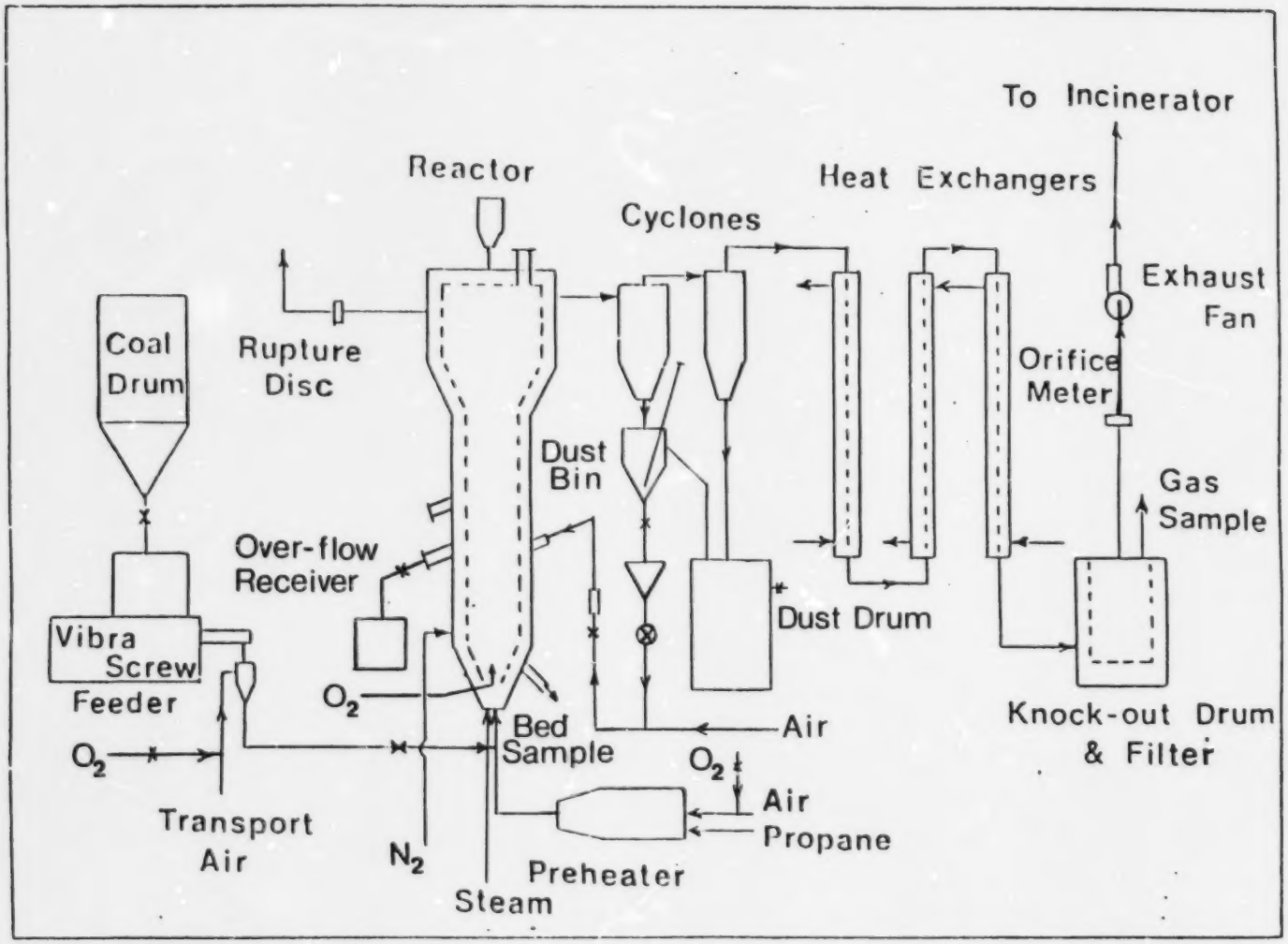

FIGURE 1

Flow Diagram of the Process Development Unit

2. Modes of Operation

Our development studies have been aimed at demonstrating the ability of the spouted bed gasifier to operate in different modes. Thus runs have been done in dry and agglomerating ash modes; with inert solids or char as the basic bed material; with oxygen or air as oxidant which implies correspondingly large or small steam flows; with and without re-cycle of cyclone char; and with a catalyst (K_2CO_3) present or absent. The array of conditions covered in the past year is given in Table 1. Detailed results for all runs are summarized in Appendix A.

About 30 runs were attempted using a typical Western Canadian sub-bituminous coal, Forestburg, and a typical bituminous coal, Balmer. Properties of the coals are given in Table 2. Particle size distributions are listed in Table A-5, Appendix A. In contrast to some previous work the intention was to make each run sufficiently long, and without mid-run operating condition changes to draw firm conclusions particularly on carbon conversion. Because of the attempt to achieve ash agglomeration which requires a fine control of temperature, flow rates and nozzle geometry, a number of runs in the exploratory stages did not meet the planned intentions in terms of running time.

Since the aims of the work this year were to examine operation with ash agglomeration, it was deemed necessary to do this in a char bed rather than in the presence of inerts. Thus all but one of the current years' experiments were done with an initial bed consisting of coal or char rather than sand or gravel.

3. Char Bed Runs with Non-Caking Coals (Task 2)

A series of runs was undertaken to study char versus inert bed operation using Forestburg coal. The run conditions are given in Table A-1, Appendix A. Inert bed runs used for comparison were carried out during the 1982-1983 and

Table 1 Outline of Operating Modes 1983-1984

Run	Coal	Ash Mode	Initial Bed	Oxidant	Char Recycle	Catalyst
88	Forestburg	Dry Ash	Char	Air	No	No
89					No	
90A					Yes	
90B					No	
91					Yes	
92					Yes	
93				Air	Yes	
94				Oxygen	No	
95					Yes	
96A					No	
96B		Dry Ash				
97C		Agglom.ash				
98						
99						
100	Forestburg	Agglom.ash	Char	Oxygen	No	No
86	Balmer	Dry	Inert	Air	No	No
101			Char	Oxygen		
102						
103						
104						
105		Dry				
107		Agglomerating				
108						No
109		Dry				Yes
110						Yes
111	Balmer				No	Yes
112		Agglomerating			Yes	No
106	Char	Dry	Char	Oxygen	No	No

Table 2 Properties of Coals

Coal		Balmer		Forestburg	
Proximate Analysis (Wet Basis)					
Moisture	(%)	1.47	1.03	23.71	12.75*
Ash	(%)	11.51	11.37	13.60	12.03
Volatile Matter	(%)	20.07	20.93	29.44	25.43
Fixed Carbon	(%)	66.95	66.67	33.25	49.79
Calorific Value	(MJ/kg)	31.24	31.47	18.15	22.86
Ultimate Analysis (Dry Basis)					
C		78.94	78.52	61.53	68.19
H		4.09	4.30	3.65	3.47
N		1.00	1.01	1.31	1.32
O		4.07	4.49	15.16	12.77
S		0.22	0.19	0.53	0.47
Ash		11.68	11.49	17.82	13.78
Runs Used		75-100	101-on	71-on	106

* Partially devolatilized

earlier contracts. Some characteristics of these experiments are shown in Figures 2-6. Runs were done with and without recycling of some of the char from the primary cyclone.

At a fixed air rate the heating value of the gas increases with coal feed rate up to about 31.5 kg/h, and then decreases (Fig. 2a). No benefit of char recycling on heating value is noted. In Fig. 2b, we see that results appear somewhat higher than 1982-1983 experience with an inert bed, and perhaps slightly but not markedly higher than the best-fit line reported for past experience.

In Fig. 3a, some evidence is noted for higher carbon conversion with char recycle at a constant value of the oxygen/feed coal mass ratio. The carbon conversion to gas includes carbon burned to CO_2, thus it increases with oxygen/coal ratio. Fig. 3b shows the typical correlation of gas heating value with oxygen to coal ratio.

The cold gas efficiency of the gasifier may be expressed as:

$$\eta = \frac{\text{G.H.V.} * \text{G.Y.}}{\text{C.H.V.}} \qquad (1)$$

where G.H.V. = gas heating value MJ/m^3
G.Y. = gas yield m^3/kg MAF coal
C.H.V. = coal heating value MJ/kg MAF coal

For a given coal, the product G.H.V. * G.Y. is a direct measure of efficiency. Previously reported results for air gasification of Forestburg coal in an inert bed gave ([4]):

$$\text{G.H.V.} * \text{G.Y.} = (221.1-29.8\ M_A/M_C) * (-0.077 + 0.062\ M_A/M_C)$$
$$= 16(M_A/M_C) - 18.5(M_A/M_C)^2 - 17.0 \qquad (2)$$

Taking the mass of oxygen present in air as $M_O = .2327\ M_A$ then

$$\text{G.H.V.} * \text{G.Y.} = 68.76\ (M_O/M_C) - 1.85\ (M_O/M_C)^2 - 17.0 \qquad (3)$$

In Figure 4, efficiency data for air gasification of Forestburg coal in char beds with and without recycle is plotted after equation (3), and oxygen-steam

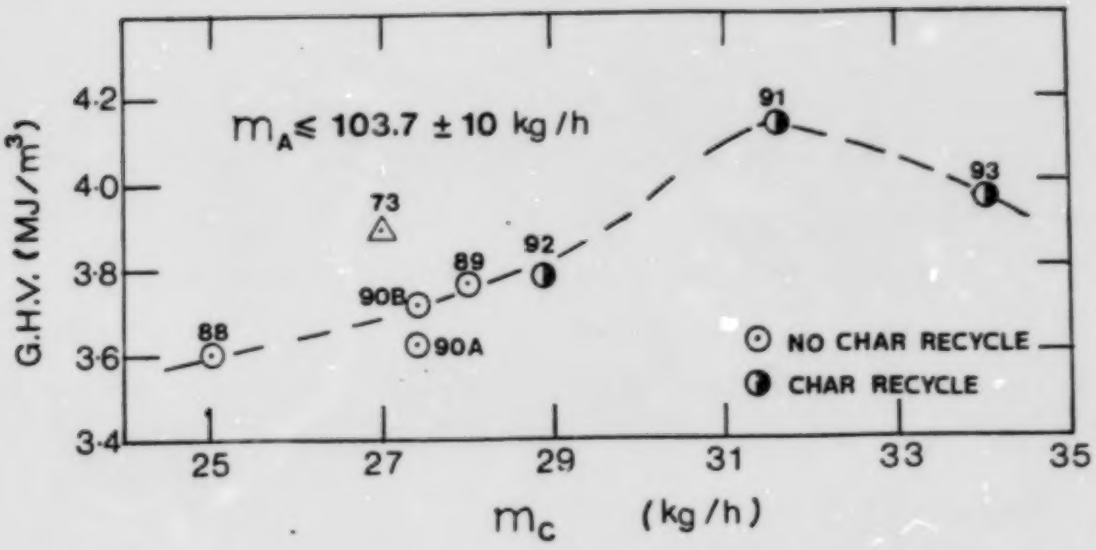

Fig. 2a Effect of Forestburg Coal Feed Rate (M.A.F. basis) on Gas Heating Value at Constant Air Rate

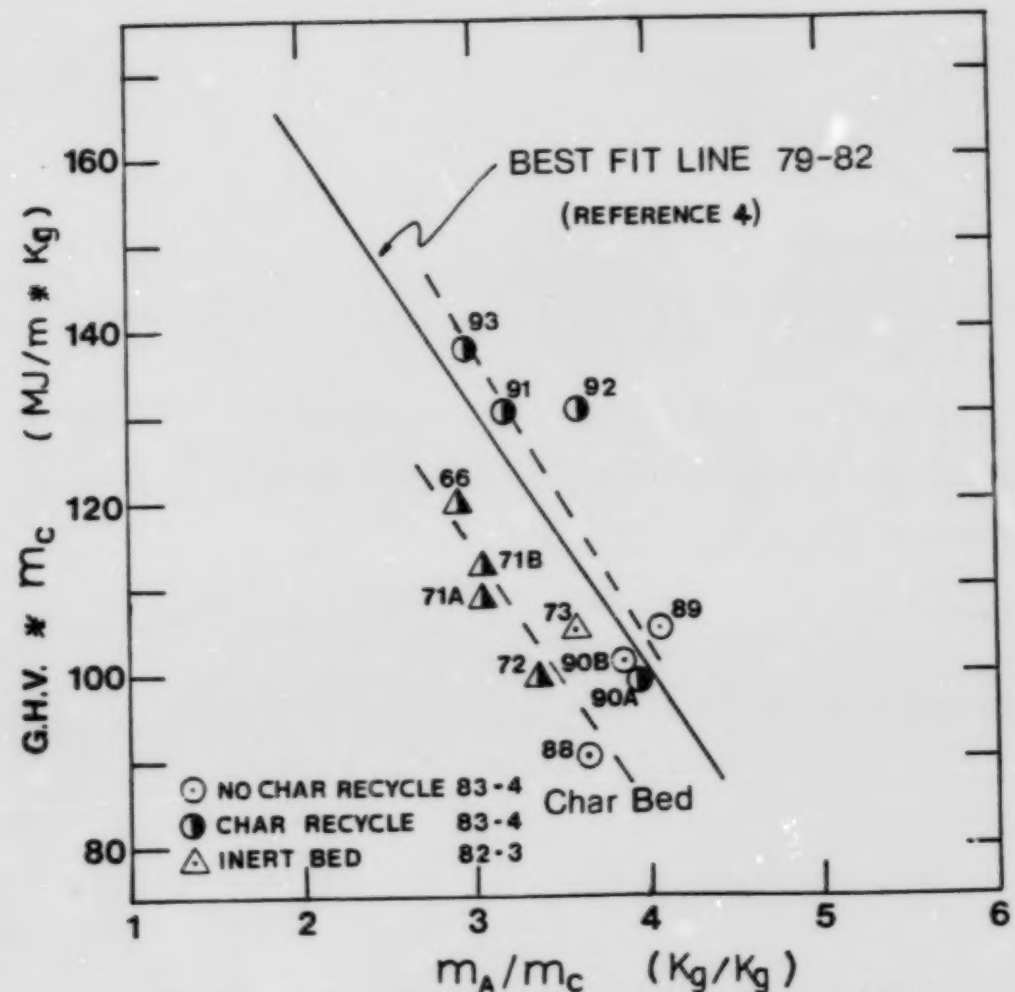

Fig. 2b Comparison of Char Bed Results with Correlation of 1979-1982 Inert Bed Data

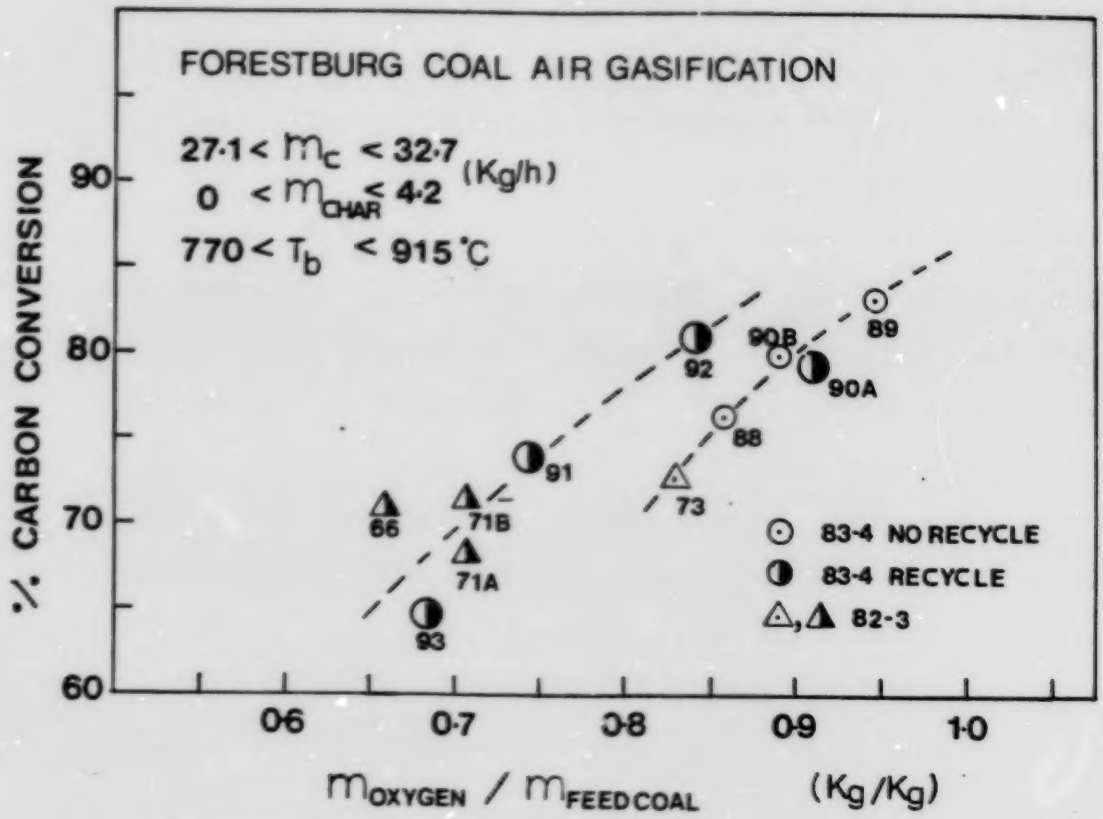

Fig. 3a Effect of Oxygen/Coal Ratio on Overall Carbon Conversion (Forestburg Coal - Air Gasification)

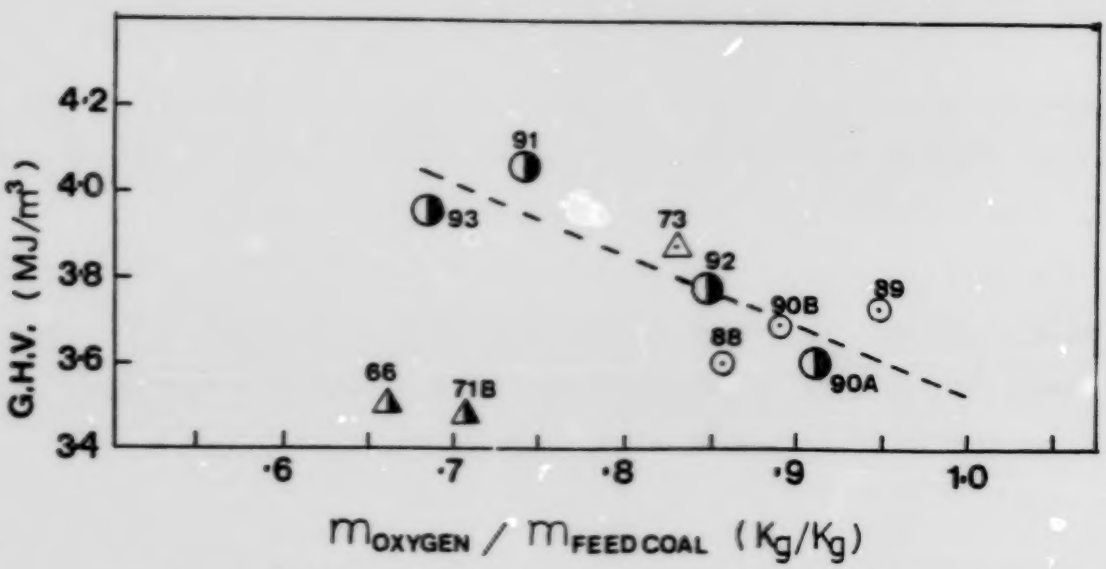

Fig. 3b Effect of Oxygen/Coal Ratio on Gross Heating Value of Gas (Forestburg Coal - Air Gasification)

gasification data for 1983-84 is included. This figure shows that both air gasification and oxygen gasification data for char beds agree well with equation (3), previously developed for air gasification only in inert beds. Results appear somewhat better than 1982-1983 results, perhaps because of differences in coal samples. Figure 5 shows that the heating value of the gas in oxygen gasification of Forestburg coal increases with the average bed temperature. At about 850°C, heating values of 9.2 MJ/m^3 are reached with gases containing typically 37% H_2, 28% CO, 30% CO_2, 3% CH_4 and less than 1% N_2.

Figure 6 shows the effect of the blast composition on the H_2/CO ratio produced. It is evident that production of H_2/CO with ratios around 2, as required for synthesis of methanol, for example require a blast of about 3 kg steam/kg oxygen with Forestburg coal, whereas to reach a value of 3, as required for synthetic natural gas, the steam/oxygen mass ratio must reach 3.6.

Overall it thus appears that operation with a char bed with air or oxygen, and with recycle of cyclone product or not is an efficient way to run the gasifier. There can be a problem with bed stability when using the char bed however, as the bed depth must be controlled. At low feedrates the bed decreases in height over time as the carbon is consumed, and the bed can be lost. This inevitably leads to large dust carryover, which is a characteristic of operation with char beds. At high feedrates it is possible to build-up the bed depth as char accumulates. The bed overflow line will eventually control this. As is evident from Table A-1, Appendix A, both of these two problems have occurred in the course of the current experiments.

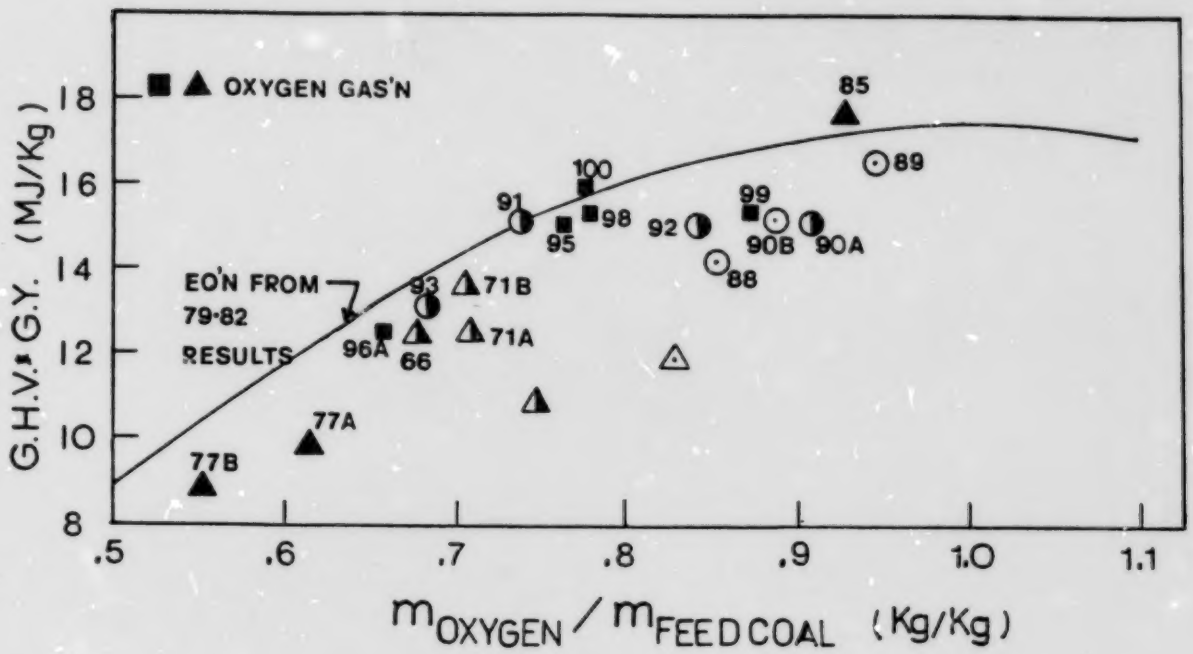

Fig. 4 Comparison of Efficiency Function for Char Bed Runs with Inert Bed Run Equation from 1979-1982. Results for Forestburg Coal (See Fig. 3a for Legend)

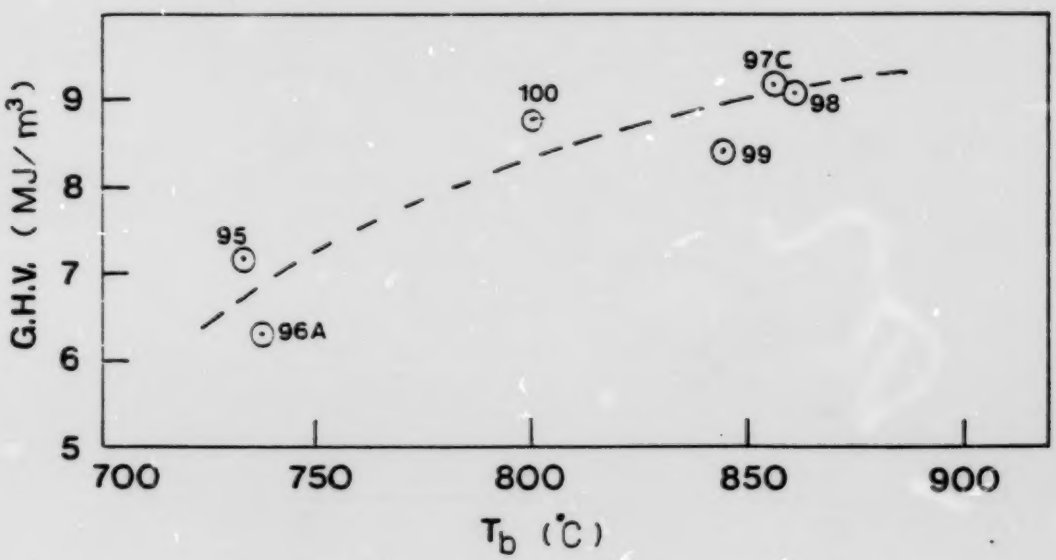

Fig. 5 Effect of Average Bed Temperature on Gas Heating Value for Oxygen Gasification of Forestburg Coal

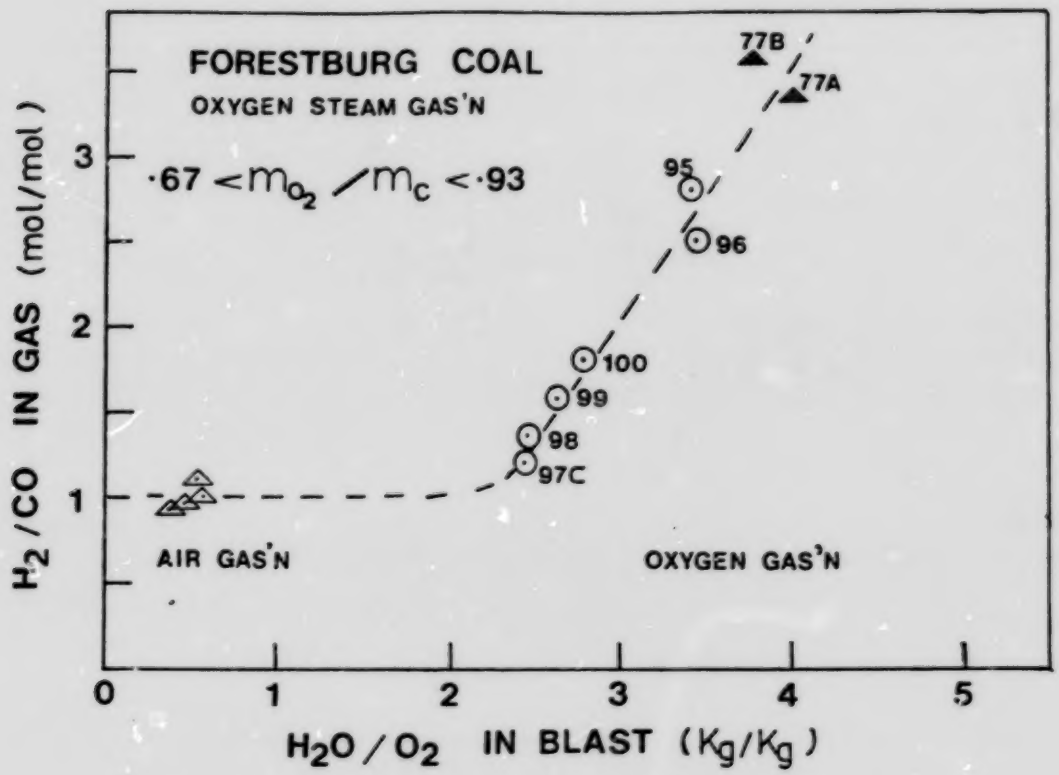

Fig. 6 Effect of Steam/Oxygen Mass Ratio in the Blast on the H_2/CO Molar Ratio in the Product Gas

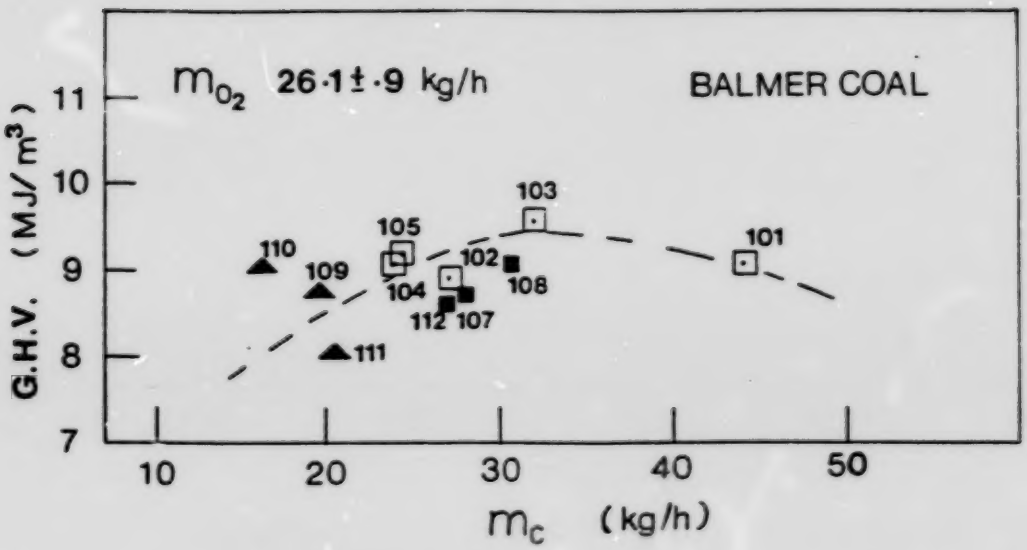

Fig. 7 Effect of Coal Feed Rate on Gas Heating Value for Oxygen Gasification of Balmer Coal
(■ Ash Agglomeration Runs ▲ Catalytic Runs)

4. Char Bed Runs-Caking Coals (Task 3)

Tests were run with Balmer coal only, and primarily with oxygen/steam blast. Figure 7 shows how the calorific value responds to increasing coal feed rate. Maximum calorific values reached here are about 9.6 MJ/m^3, giving a gas containing 37% H_2, 30% CO, 29% CO_2 , 3.7% CH_4 and no N_2. Balmer data correlate in the same manner as Forestburg coal with O_2/coal ratio (Figure 8), giving a good straight line fit.

The results can also be plotted versus bed temperature, as in Fig. 9, where carbon conversion with no cyclone char recycling reaches about 73% at the highest operating temperature used. Fig. 10a shows essentially no effect on calorific value of temperature per se, because of the different combinations used to achieve the temperature. The efficiency factor, G.H.V. * G.Y., can be smoothly correlated with average bed temperature as in Figure 10b, or versus oxygen/coal ratio. Figure 11 shows a plot of the gas molar composition H_2/CO versus H_2O/O_2 ratio. Under essentially all conditions, the molar ratio of H_2/CO is virtually unity in sharp contrast to the behaviour of Forestburg coal as shown in Fig. 6.

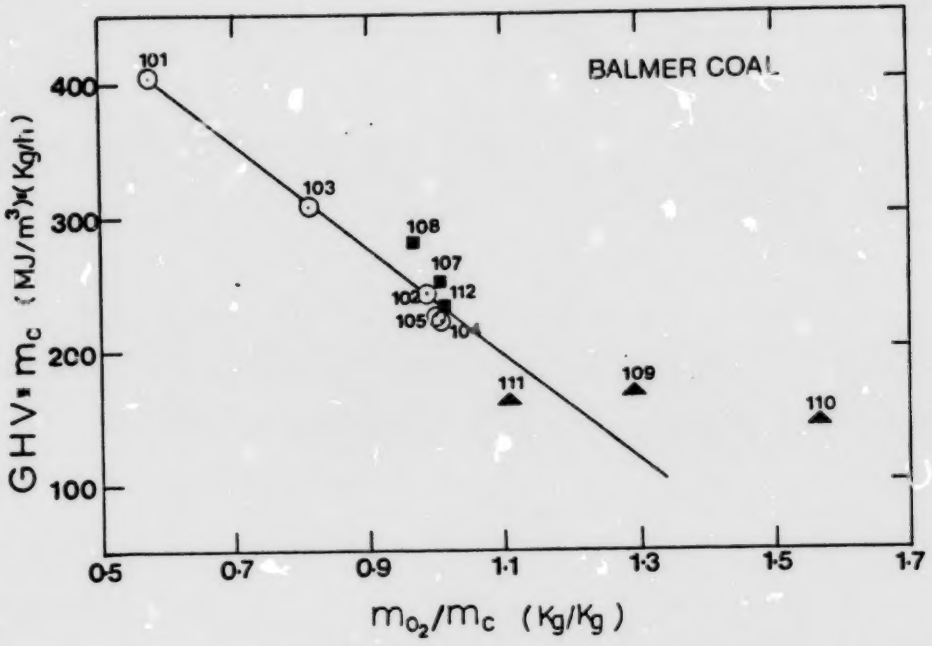

Fig. 8 Correlation of Balmer Results for Oxygen Gasification
(■ Ash Agglomeration Runs ▲ Catalytic Runs)

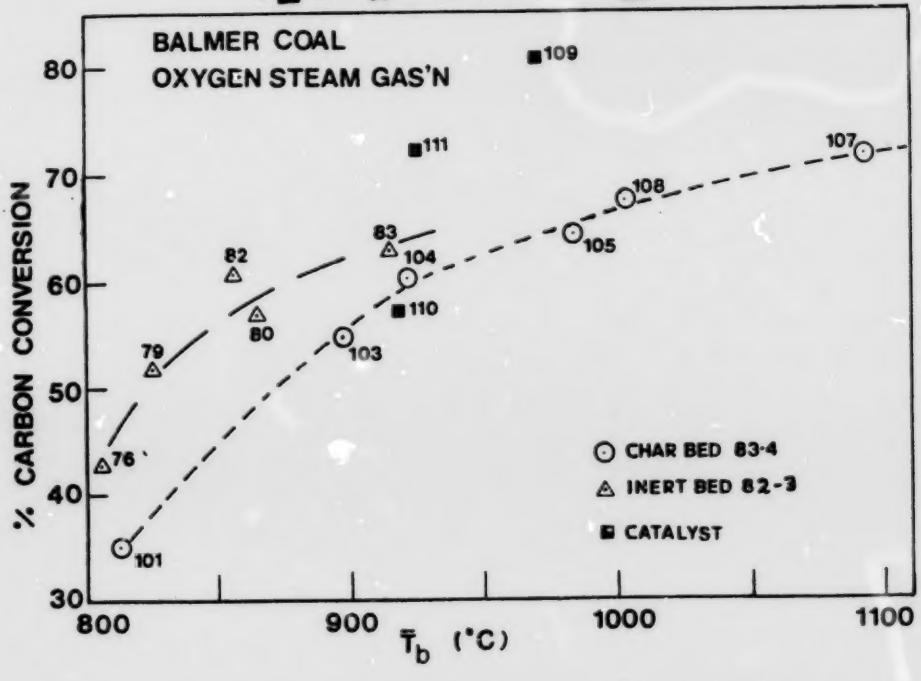

Fig. 9 Carbon Conversion versus Average Bed Temperature

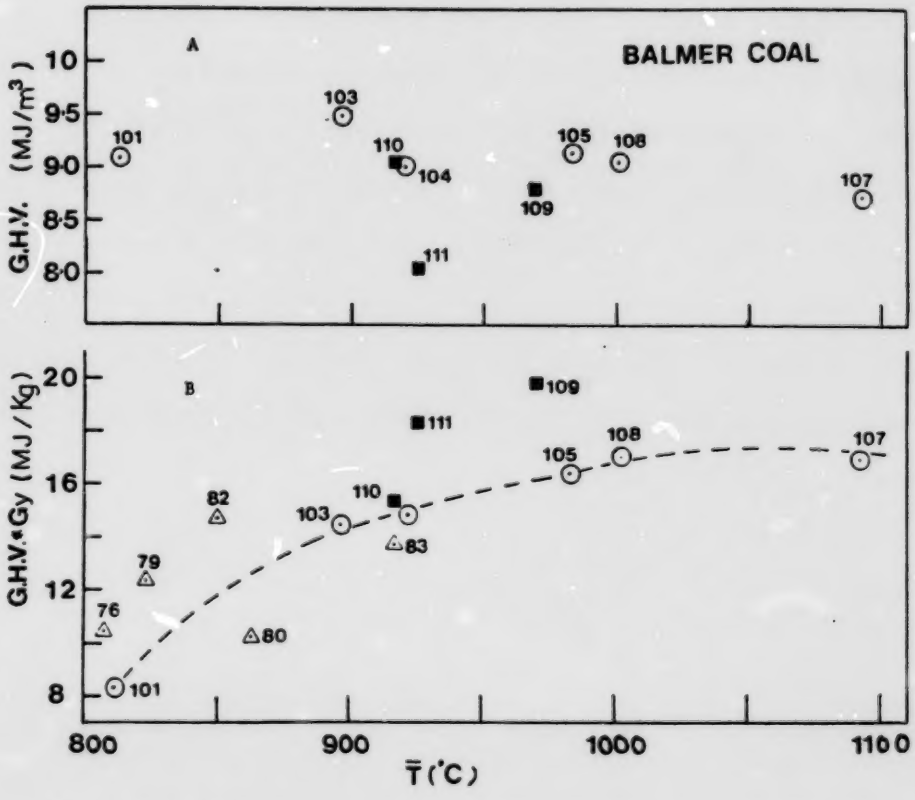

Fig. 10 Gas Heating Value (a) and Efficiency Factor (b) versus Average Bed Temperature

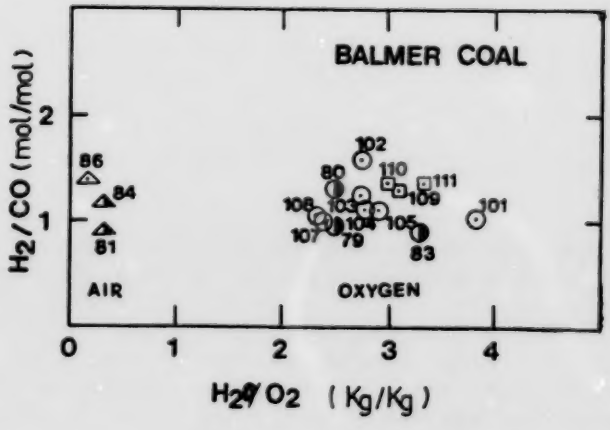

Fig. 11 Effect of Steam/Oxygen Mass Ratio in the Blast on Hydrogen/Carbon Monoxide Molar Ratio in Product Gas (see Fig. 9 for legend)

5. Agglomerating Ash Runs (Tasks 4 and 5)

Operation in the ash agglomeration mode requires a temperature in the agglomerating zone sufficiently high to render the ash particles sticky, but not so high as to produce slagging, which could result in a single large lump. In order to remove agglomerated material of a controlled size from the bed, the zone of agglomeration must be properly located, and provision made for the agglomerates to exit the reactor. In the present case agglomeration was induced by use of oxygen to produce a local high temperature zone. A series of evolutionary changes were made to the flow piping and flow rates in the conical bottom of the reactor in order to achieve agglomeration. These changes are described step by step below The initial trials were done with -4 +16 mesh Forestburg coal (Table A-4, Appendix A).

Run 97a

The ash agglomerating oxygen was piped to the reactor cone by eight 1/4" s.s. tubes. The inlets were spaced at equidistant points around the cone, as shown in Fig. 12a.

The reactor was charged with 23 kg of char and the char bed heated to 500°C by the oxygen free flue gas from the propane burner. Initially 13 kg/h of Forestburg coal was fed to reactor. This was gradually increased to 50 kg/h. Air, 50.4 m^3/h, is used as the main spouting fluid during start-up but it is gradually replaced by pure oxygen and steam, at flowrates of 15.0 m^3/h and 48.0 m^3/h respectively. The propane burner was shut off as the bed temperature increased from 500°C to 750°C.

After about 1 1/2 hours a reasonably steady condition reached which was confirmed by gas chromatograph analysis. Pure oxygen was introduced to the eight ports at the side of the reactor cone. Two ash agglomeration oxygen flowrates were attempted, 1.18 m^3/h and 2.24 m^3/h. After 15 minutes the oxygen flowrate decreased below the desired value and the run was stopped after 2 hours of total run time.

The reactor cone was lowered and removed from the reactor. Six of the oxygen ports were blocked with used ash and char and two of them had to be replaced because the tips were burnt out. One of two remaining open tubes had a blue discoloration about 0.5 m from the inlet indicating hot coal had dropped into the tube and started burning. During the experiment, a hot spot was discovered at one of the oxygen pot nipples indicating the refractory had to be repaired. No ash agglomerate was found in the bed char, 17.7 kg.

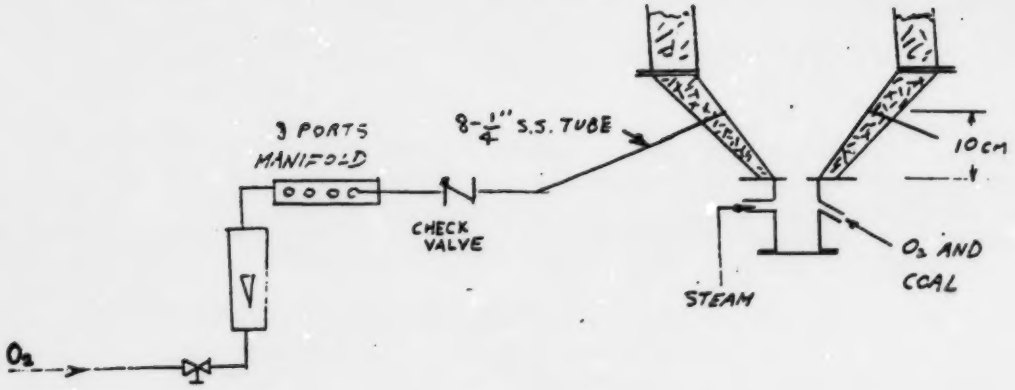

Fig. 12a Sketch of 8-Port Oxygen Inlet for Agglomeration

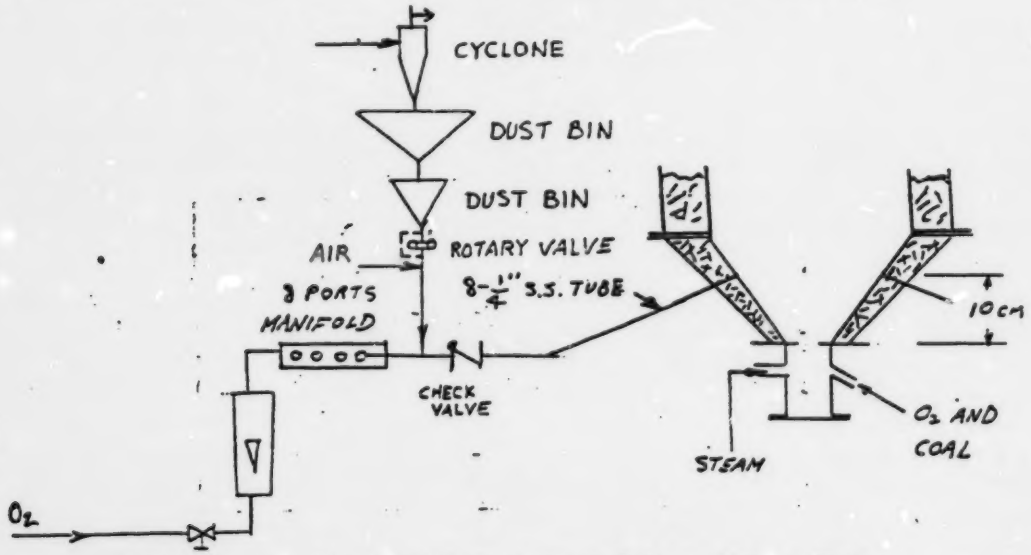

Fig. 12b Air line Modification to 8-Port Oxygen Inlet

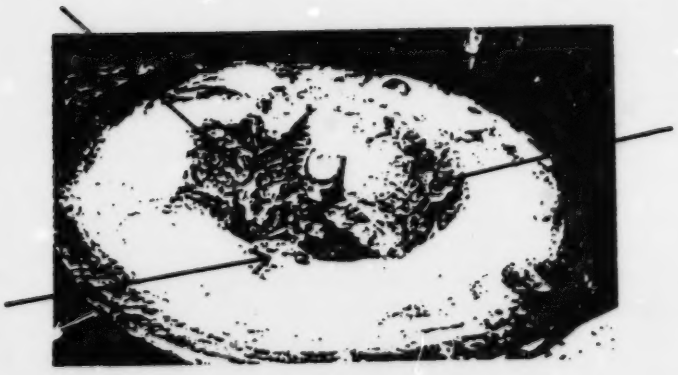

Fig. 12c Deposits on Oxygen Ports (Run 97b)

Run 97b

From run 97a the ash agglomerate oxygen rotameter float was found to be too light and was replaced with a heavier one. The cone refractory was repaired. To prevent the oxygen ports from blockage an air line was connected to the existing oxygen line by using a tee. Air was blown continuously into the reactor until oxygen was used (Fig. 12b).

The coal, oxygen and steam flowrates were 50 kg/h, 15.0 m^3/h and 54.0 kg/h respectively. O_2 flow to the port was increased from 1.6 m^3/h to 3.0 m^3/h to try to increase the bed temperature to 1150°C locally. TC#4 indicated 760°C which is also the average bed temperature. The location of TC#4 is not close enough to the injection port to measure the true temperature.

The run ran smoothly until the hot char in the cyclone dust bin was ignited by O_2 seeping past the rotary valve and the ball valve. The run had to be terminated.

The cone section was removed from the reactor. Very little loose ash agglomerate were found in the bed. At each of the eight oxygen ports a small patch of clinker was formed (Fig. 12c) and the largest one measured 3.8 cm dia. x 1.90 cm high. The clinkers had a porous and glassy structure.

Run 97c

It was decided to attempt to feed the agglomerating oxygen into the centre of the spout rather than via the periphery of the cone. The eight oxygen injection ports were therefore replaced by a single 1/4-in. s.s. tube located at the centre of the port and 14.6 cm above the inlet orifice. The air to the oxygen injection port was tapped directly from the main air line by passing the dust collecting bin. Thermocouple #4 was located 14.6 cm from the refractory wall and 9.5 cm above the oxygen injection port inlet (Fig. 13a).

The average bed temperature during the run was 858°C and the temperature measured at TC#4 was 1150°C. When the reactor was opened for examination, three distinct zones of bed material were observed at the reactor cone (Fig. 13b and 13c). As seen in Table 3 Type I material consisted of fine coal dust located near the orifice and the cone wall.

Type II material consisted of large particles ranging from 0.5 cm to 2.5 cm in size and were found mostly beneath the O_2 injection tube. They are formed by fine ash fused together. Type III have a mean particle diameter of 2.34 mm and are found mostly above the O_2 injection port. They are grey in colour on the surface but when they are cross sectioned, black coal is exposed beneath the grey surface.

Run 98

Run 98 was performed using the same set-up as Run 97c to try to duplicate this run. The run conditions were similar except for the coal feed rate, 55.80 kg/h (wet basis) instead of 47.40 kg/h (Table A-2, Appendix A). Run 98 had to be stopped after 2.2 hrs due to pressure build-up in the coal feed line ($p > 4.5$ psig). When the cone was lowered, a large amount of moist coal fines were found at the orifice inlet.

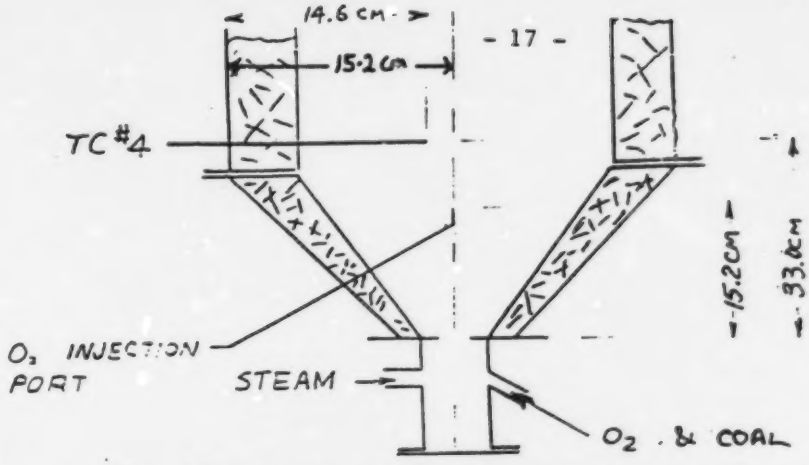

Fig. 13a Single Oxygen Inlet Port for Run 97c

Fig. 13b Photograph of Materials of Type I, II and III (Run 97c)

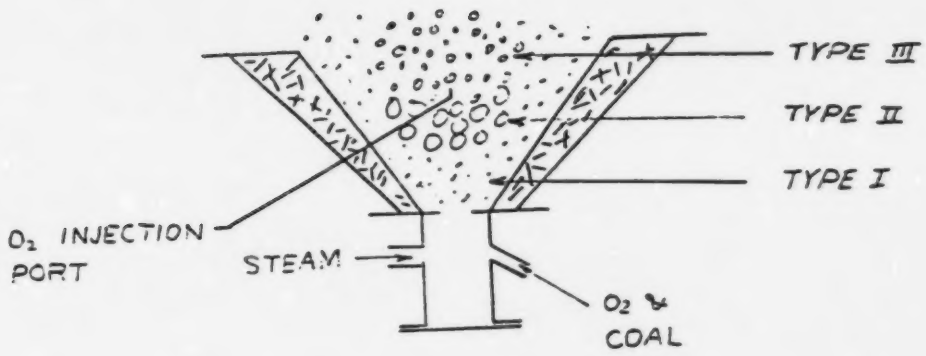

Fig. 13c Location of Materials of Types I to III (Run 97c)

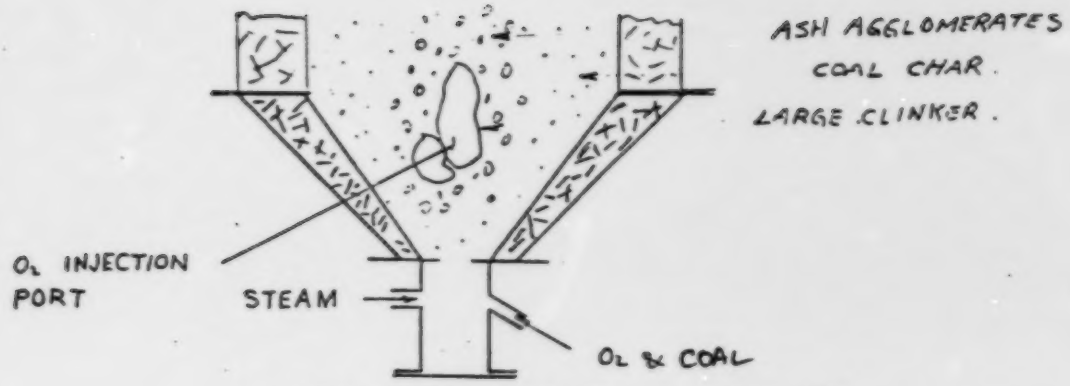

Fig. 13d Location of Agglomerates (Run 98)

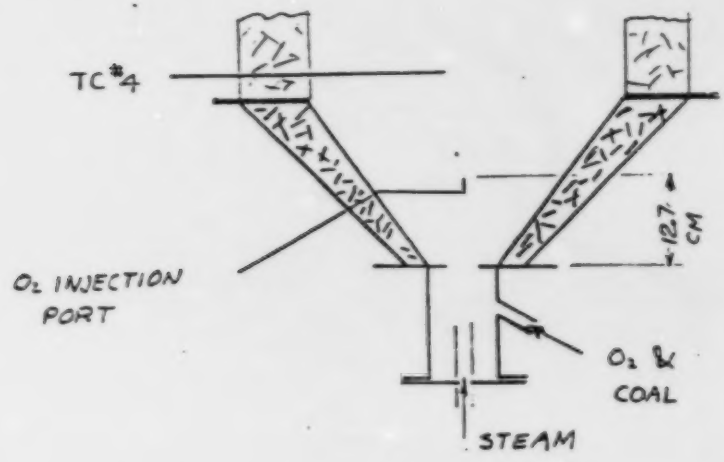

Fig. 13e New Piping Arrangement for Steam (Contrast with Fig. 13a)

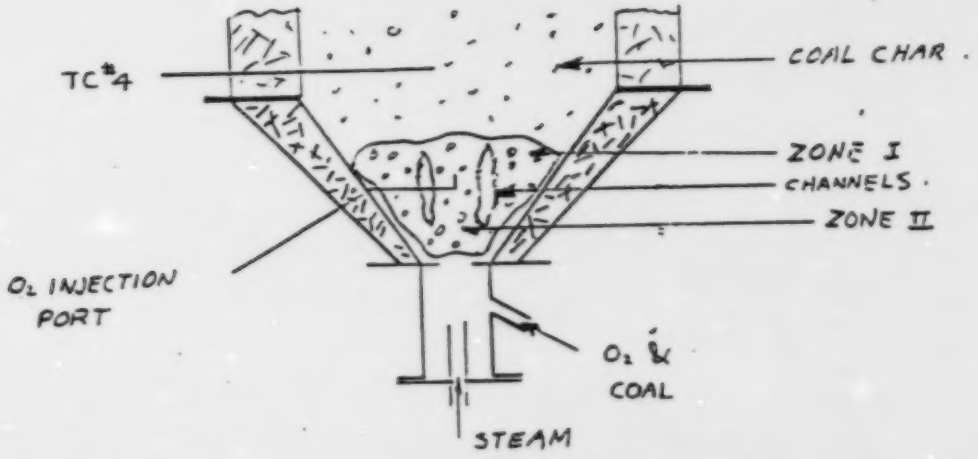

Fig. 13f Sketch of Agglomerates (Run 99)

TABLE 3: Run 97c Ash Agglomeration Run with O_2 and Steam

Carbon Content Analysis

Type	% Carbon	Remarks
1	38.57	Forestburg coal collected around the cone
2	1.60	Ash agglomerates collected around the O_2 inlet
3	4.44	Ash agglomerates collected above the O_2 inlet

TABLE : Screen Analysis of Type I and Type II Particles

Ave. Opening (mm)	Type I wt %	Ave. Opening (mm)	Type II wt %
3.36	1.23	3.36	12.14
2.87	2.67	2.68	66.01
2.19	2.26	1.60	17.45
1.84	2.67	1.02	2.79
1.54	2.88	0.72	0.90
1.30	3.50		
1.02	9.67		
0.72	44.65		
0.47	5.14		
0.28	18.72		
0.21	6.58		
dp (mm)	0.53		2.34
Particle density (gm/cc)			3.65

The majority of ash agglomerates were at the centre of the bed and were mixed with char particles (Fig. 13d). Fine char powder was found mainly at the bottom of the cone and at the side of the bed. Two large clinkers (16.5 cm Lx 3.8 cm W, 5.1 cm L x 1.9 cm W) were found at the O_2 injection port.

Run 99

The ash agglomeration oxygen inlet was moved closer to the orifice. The saturated steam inlet was re-located to directly below the orifice to facilitate coal transport into the bed (Fig. 13e). Relocating the main steam line seemed to alleviate the coal clogging problem at the bed entrance. Less coal dust was found after the run.

A large ash agglomerate of 1.6 kg was found at the cone with 8.2 kg of char sitting above the agglomerate. There was little or no ash agglomerate in the char. There were two observed zones in the large ash agglomerate (Fig. 13f).

Zone 1 consisted of loosely packed white ash particles fused into a porous mass. The particles could be separated fairly easily by hand. The particle size ranges from 0.5 mm to 1.5 mm.

Zone 2 located at the centre of the ash agglomerate where the O_2 injection port is located. It consisted of brown molten ash with large channels (≈ 0.5 cm ϕ to 1.0 cm ϕ) running vertically. At the undersides of the channels the molten ash had a glassy and shiny appearance and it was very difficult to break by hand.

The ash agglomerate is suspected to have formed very early in the run given the temperature profiles.

Ash agglomeration runs were attempted also with Balmer coal (Table A-4, Appendix A), using the same geometry ofoxygen and steam inlet of Fig. 13e. Run 107 was the most successful of these runs, and spherical agglomerates of about 5 mm containing less than 1% carbon were produced (Fig. 14). These agglomerates were collected from the bottom of the cone. The temperature in the agglomerating region was about 1150°C. Further attempts were less successful because of temperature problems (Run 108).

The ash agglomeration trials can be summarized as follows:

(i) A suitable geometric arrangement to produce successful ash agglomeration has been achieved through a series of evolutionary changes,

(ii) Good spherical, low-carbon agglomerates have been produced using Balmer coal. Temperatures in the agglomerating zone must be ~ 1150°C. For

Forestburg coal some less successful agglomeration was achieved probably because the temperatures were insufficiently high.

(iii) Continuous outflow of agglomerates will require further modifications to the cone section and has not been demonstrated.

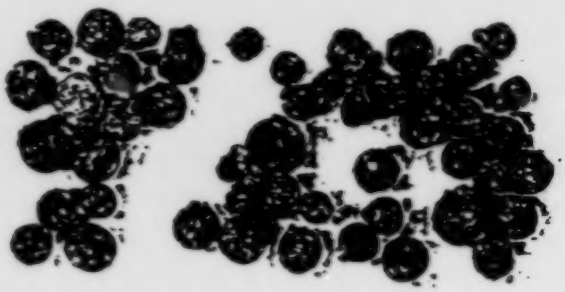

Fig. 14 Ash agglomerates produced from Balmer Coal
(Run 107 - actual size)

6. Sulphur Balances in Gasification (Task 7)

The aim was to reduce the sulphur content of the off-gas by injecting limestone or dolomite into the bed. A new gas chromatograph with a flame photometric detector was installed to analyse for sulphurous compounds. Two standard calibration curves were prepared for H_2S and SO_2. A simple gas sampling system (Fig. 15) was set up and used for a series of Balmer coal gasification runs (Run 107-112).

The sampling system consisted of an ice-bath, two one-litre glass flasks, and a glass column filled up with glass wool. The purpose of using an ice-bath is to cut down the existence of fine dust and moisture of the flue gas. Two gas samples were taken roughly every 15 minutes for the G.C. analyses. The condensate solutions trapped in the flasks were filtered after the experiment and diluted to the nearest volume with an addition of 5 ml 3% H_2O_2 solution. The sample solution was adjusted to pH between 2.5 to 4.0 with perchloric acid; 2 drops of 2% thorin indication was added and titrated with barium perchlorate solution, taking the change from yellow-orange to pink as the end point. No obvious colour change was found from the titrations, therefore no SO_2 was found in the condensate solutions.

Table 4 shows average H_2S and SO_2 levels in the gas for a series of runs. In normal gasification the Balmer coal, the H_2S level is about 240-380 ppmv, and that of SO_2 1-4 ppmv. For the catalytic runs where loadings of K_2CO_3 are added to the coal, the H_2S level was undetected in two runs and about 33 ppmv in the third. No SO_2 could be detected. Detection limits with the current FPD are below 1 ppmv.

Calculations show that about 30-40% of the incoming sulphur reports to the gas. Since no sulphur was detected in the condensate from the wet gas it must be assumed that the remainder reports in the char. Because of a

temporary breakdown in the sulphur analyzer of the UBC Forestry Faculty, the latter fact could not be confirmed at the time of writing. Sulphur balances will be completed once the sulphur levels in the char can be determined.

Little work was done on particulates in the gas phase as the Scientific Advisor who originally proposed the joint work with ERL had been transferred to another project. In Table A-5, Appendix A the size distribution of the dust which escapes the cyclone is reported for one run.

Table 4 Sulphur Levels in Gases in Balmer Coal Gasification

Run No	Mode of Gasfication	Conc'n in Gas (ppmv) H_2S	SO_2	Percent of S in Gas (wt %)
107	ash agglomeration	240	2.7	30.2
108	ash agglomeration	343	3.6	41.4
109	catalytic	33	-	
110	-	Not detected		
111	-	Not detected		
112	ash agglomeration	378	0.9	

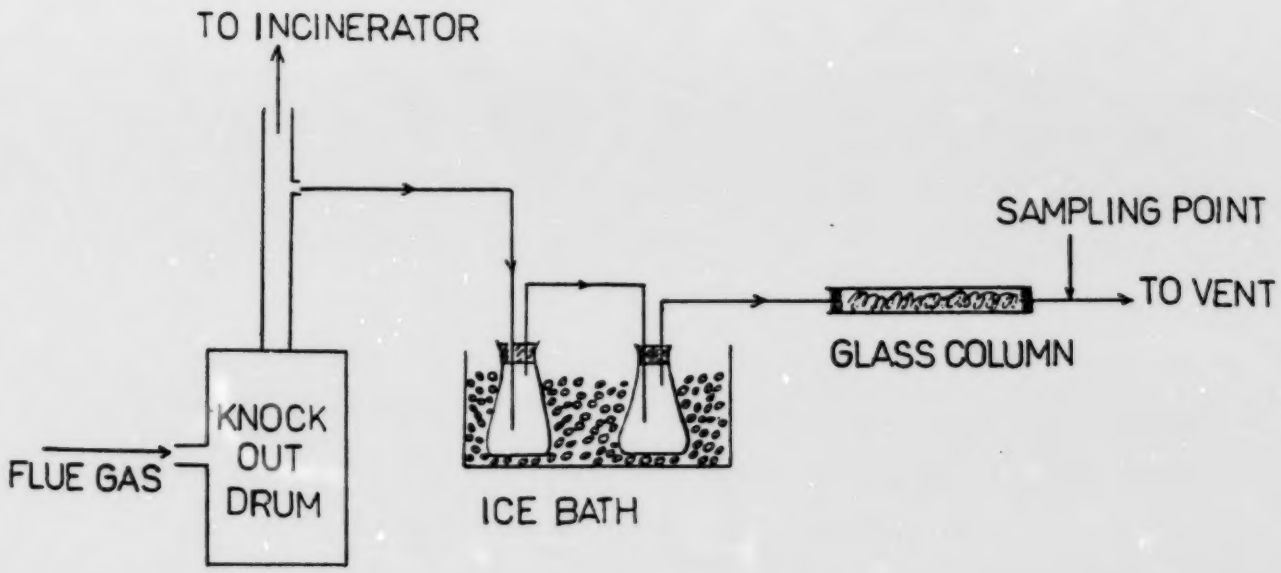

Fig. 15 Schematic of Sulphur Analysis Sampling Train

7. Catalytic Gasification Runs (Task 6)

The aim of these preliminary tests was to see if potassium, a known catalyst, applied as potassium carbonate, would be effective in improving carbon conversion, or efficiency at a given temperature.

a) Preparation and analysis

Three drums of Balmer coal were prepared for the series of catalytic coal gasification runs. Balmer coal, with nominal levels of 15 wt% and 30 wt% of potassium carbonate was prepared. Potassium carbonate powder was dissolved in ordinary tap water to form a saturated solution, which was sprayed onto the coal in repeated applications. The wet coal was spread over a steam-heated floor to dry. The temperature controller was set at 30°C. The wet coal took about two full days to dry. During the drying the coal agglomerated. Two drums of Balmer coal, with high potassium carbonate content and one drum of Balmer coal with less potassium carbonate content were prepared. It was necessary to verify the potassium loadings on the coal: this is described below.

A simple test was performed to find out the absorption rate of potassium carbonate solution on the Balmer coal. Samples of 500-gm Balmer coal were soaked in three different concentrations of potassium carbonate solutions over a period of time. The samples were then filtered by a simple filtration process. The filtrates were collected and sent to a commercial laboratory. The results were summarized as shown in Table 5. At the same time, two samples of pure potassium carbonate were put in the crucibles and heated up in the oven for four hours. Therefore, the moisture content within the potassium carbonate would be determined. The average moisture content of the potassium carbonate itself was found to be 0.77%.

b) Results of Potassium Loading Tests

The initial weights of coal and potassium were recorded before the preparation began. The final weights of the three drums of catalytic Balmer coal were registered after the drying process. Since potassium carbonate is a strong hygroscopic substance, it absorbs the free moisture from the atmosphere. In order to get an accurate measurement, two catalytic coal samples were placed into the oven at 325°F to get rid of any remaining moisture. Hence, the wt% ratio of potassium carbonate to Balmer coal (wet basis) could be found. The wt% ratio of K_2CO_3/Balmer coal with nominal levels of 15 wt% and 30 wt% were found to be 11.66% and 21.88% respectively. The results are summarized in Table 5.

In order to confirm these results a small leaching test was performed to find out the potassium carbonate content in the coal. A sample of 500 grams with 11.66 wt% of K_2CO_3 was placed in a beaker of warm water at 70°C. The solution was simply tested by a piece of alk-acid test-paper and the colour change was observed. This simple procedure was repeated until the colour of the test-paper changed from blue (pH ≈ 10) to pale green (≈ 8). The sample was then filtered and the final residue was put into the oven to get rid of any remaining moisture. The sample was heated at 325°F for approximately 10 hours, and the sample then reweighed, and the amount of potassium carbonate could be calculated by the difference in weight. This procedure gives a check on the previous calculation. The percentage recovery of K_2CO_3 from the coal by the leaching process was found to be 91.7%.

c) Catalytic Gasification Trials

Three catalytic gasification runs were attempted (Table A-3, Appendix A). Before discussing the effects in detail it is critical to note that the adhesion of agglomerate of the carbonate treated coal made necessary a further

crushing step to break these agglomerates. Thus the particle size as fed was markedly different from that of the original coal. Thus the original coal was typically 1.6-mm mean particle diameter (Table A-6, Appendix A) whereas the 21.9% K_2CO_3 loaded coal used in Runs 110 and 111 averaged 0.6 mm in mean particle diameter. The less highly loaded coal of Run 109, at 12.1% K_2CO_3 was 1.3 mm in size. It has been established previously that smaller coal size leads to poorer performance.

Results for the three runs are listed in Table A-3, Appendix A, and are plotted in the earlier plots with other Balmer coal data. In Figs. 9 and 10 it is clear that Run 109 is higher in carbon conversion and efficiency factor by about 15%-20% for the catalytic run at the same average bed temperature. At the higher potassium carbonate loading of ~21.9%, Run 110 shows the penalty paid by the reduced particle size, as the carbon conversion and efficiency are roughly that expected for the un-treated coal. Because of the large carbon carryover for such small feed sizes, it is essential to recycle char from the cyclone. Data for Run 111 where this is done restores the carbon conversion and efficiency gains to levels comparable to those of Run 109, in spite of the 0.6 mm average feed size. Essentially the same effects are noted in the performance parameters of Fig. 7, and Fig. 8 for the three runs.

There is a price to be paid, then for the presence of the K_2CO_3 on the coal, in that to feed the coal easily, some extra agglomerate crushing is required. The hygroscopic nature of the salt also causes problems at the feed point, where plugging is apt to occur due to the re-agglomeration or pick-up of steam by the carbonate on the coal surface. All three catalyst runs were bothered by feeding problems.

A further advantage of the presence of K_2CO_3 lies in the sulphur content of the produced gases. Table 4 shows no detectable sulphurous species in the

gas for the catalyst runs. Sulphur capture may well occur as the K_2CO_3 decomposes to K_2O which would react rapidly with the H_2S in the gas yielding potassium sulphide.

These few tests on catalytic gasification then show a combination of advantages and disadvantages to the application of K_2CO_3.

Table 5 Potassium Carbonate and Moisture Content of Treated Coals

Nominal (Target) Wt% K_2CO_3 on Coal	15	30
% H_2O in Coal	4.23	2.05
Net Wt K_2CO_3 (lb)	43.56	171.18
Net Wt Balmer Coal (Wet Basis) (lb)	359.5	953.4
Moisture absolved by K_2CO_3 (lb)	13.94	9.72
Actual Wt% K_2CO_3 on Coal (Wet Basis)	11.66	21.88

8. In-Bed Gas Composition and Temperature Profiles

This part of the work was carried out by M.A.Sc. student Zaki Haji-Sulaiman, under the co-supervision of Dr. C.J. Lim and the Principal Investigator.

A set of gas sampling probes and a sampling train were constructed (Fig. 16 + 17) and a series of ports drilled through the gasifier lining (Appendix B). During a series of runs, samples were taken, stored in syringes and analyzed via the gas chromatograph at the end of each run. Sampling velocities were based on an approach to isokinetic sampling using velocity profiles calculated from equations available in the literature. Sampling points are shown in Fig. 18.

Typical profiles in air gasification of Forestburg coal are shown in Figure 19a-c. Near the wall, in the gasifier annulus (Fig. 19a), the oxygen concentration is seen to drop to zero about 0.1-m above the inlet orifice. H_2 and CO concentrations rise smoothly and rapidly to values of about 24% near the top of the bed. The local CO_2 concentration goes through a minimum at the top of the conical section. In Figure 19b, midway through the annulus, a similar oxygen profile as in (a) is set-up. A somewhat different profile exists for H_2 and CO with a point of inflection near the top of the conical section of the column. The relatively flat CO_2 profile matches that of oxygen. In Fig. 19c, near the centre of the column, and in the spout region the oxygen concentration persists to about 0.35-m of height rather than dropping to zero near the orifice as in the annulus. The CO_2 profile is the mirror image of the oxygen profile. H_2 and CO show no significant presence until the oxygen has dropped to about 2%, 0.35-m from the orifice. In general these profiles show that for air gasification,

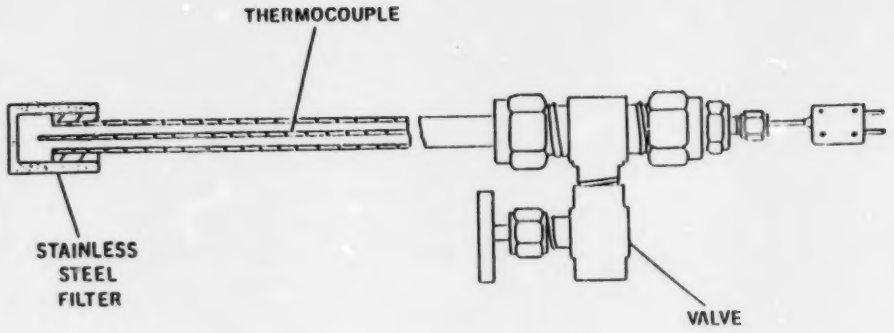

Figure 16 - Gas sampling probe.

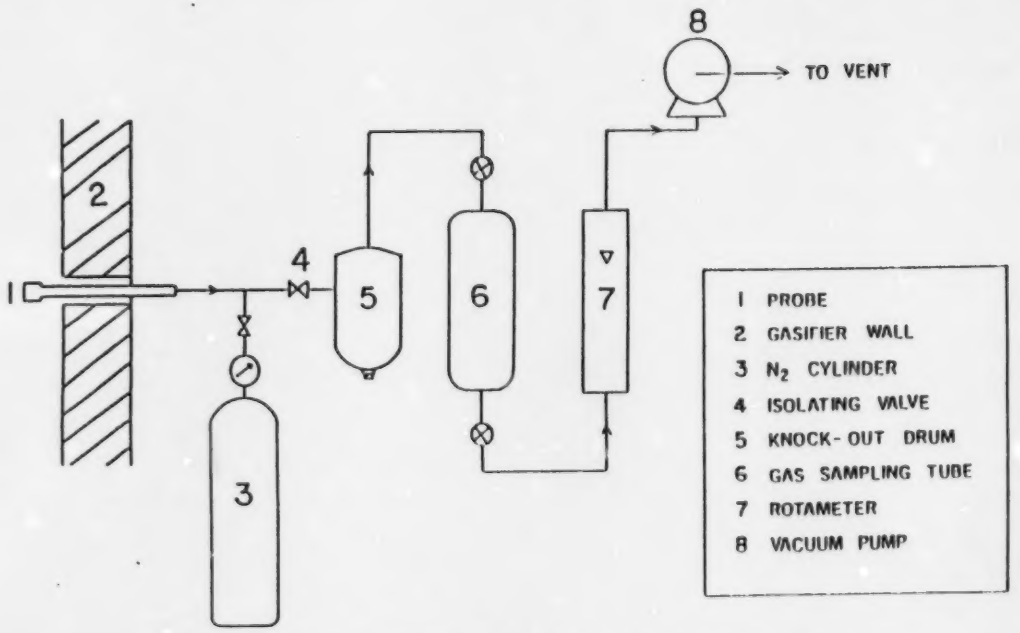

Figure 17- Schematic flow diagram for the gas sampling line.

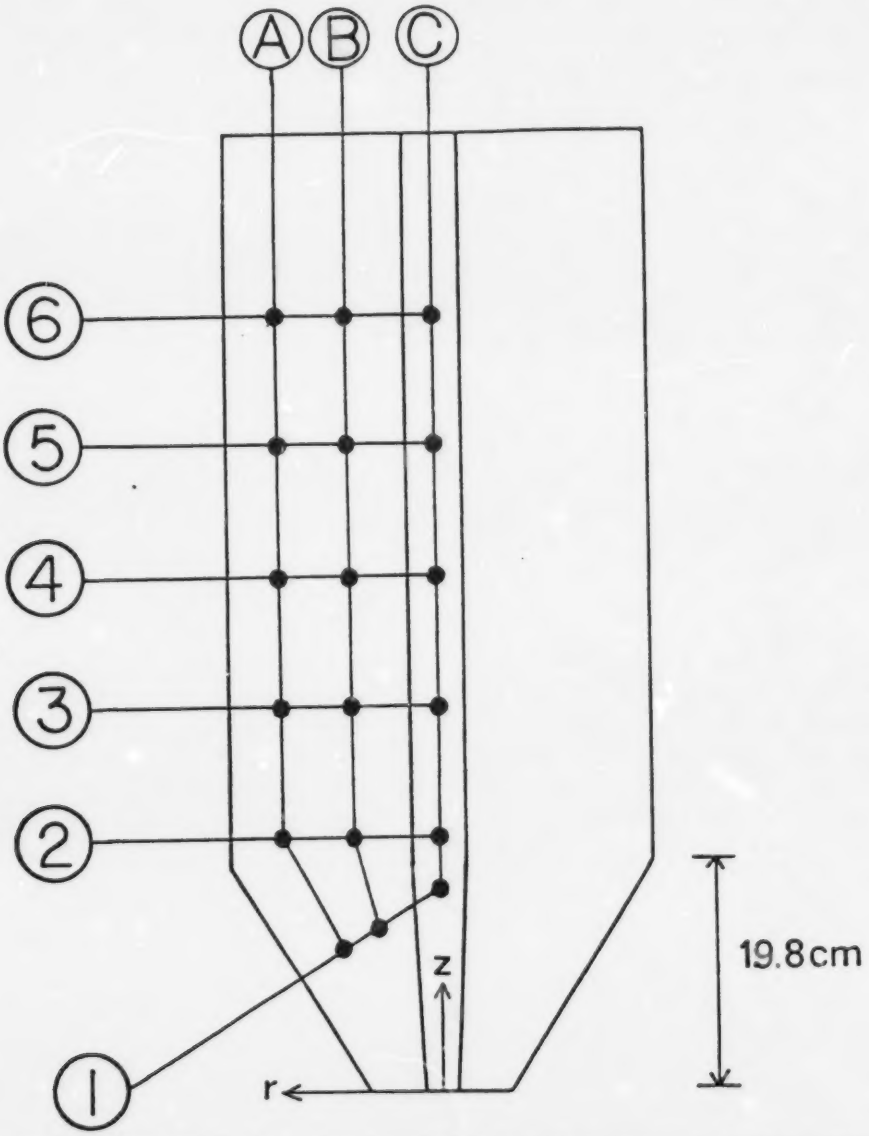

No.	z (cm)	r (cm)	No.	z (cm)	r (cm)	No.	z (cm)	r (cm)
6A	65	11.4	4A	45	11.4	2A	25	11.4
6B	65	6.3	4B	45	6.3	2B	25	6.3
6C	65	0	4C	45	0	2C	25	0
5A	55	11.4	3A	35	11.4	1A	8.5	5.0
5B	55	6.3	3B	35	6.3	1B	9.1	4.0
5C	55	0	3C	35	0	1C	11.4	0

Figure 18 - Locations of sampling points in the bed.

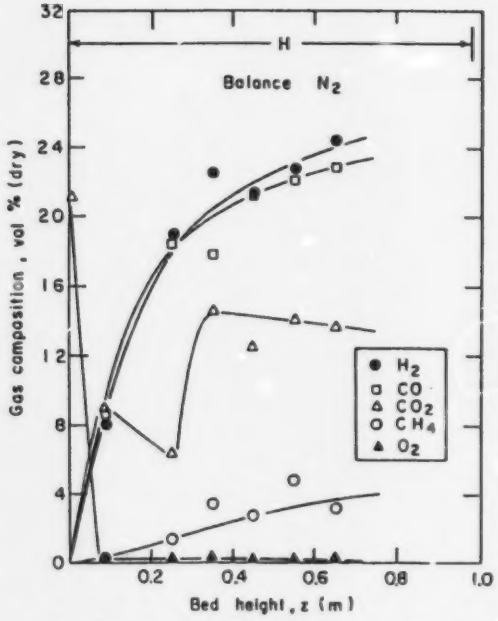

Figure 19a - Axial gas composition profiles along position A for the Forestburg coal-air system (Run 93).

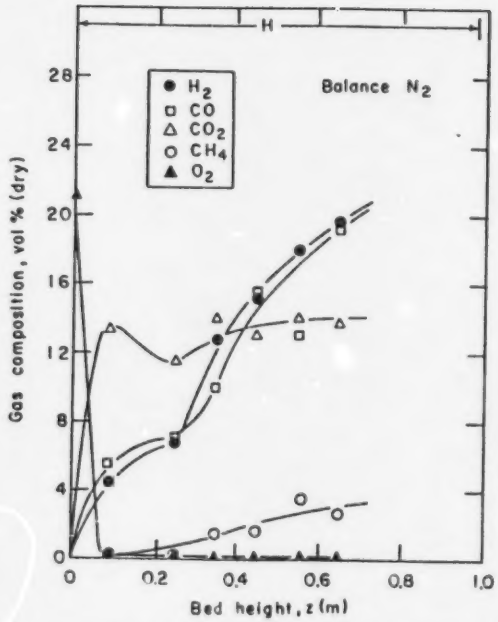

Figure 19b - Axial gas composition profiles along position B for Forestburg coal-air system (Run 93).

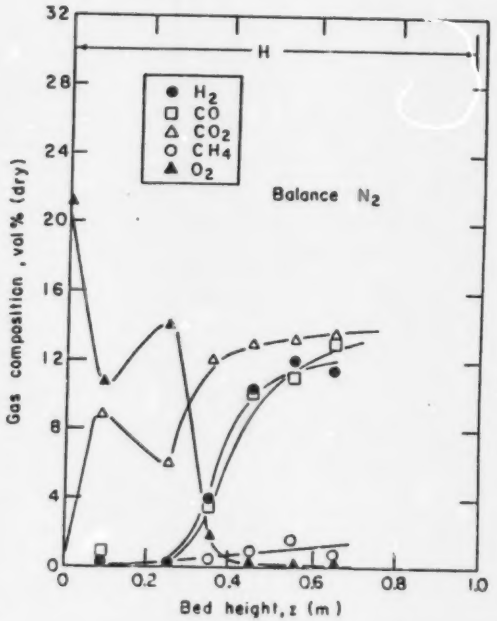

Figure 19c - Axial gas composition profiles along position C for the Forestburg coal-air system (Run 93).

(a) the oxidizing zone is in the spout region only, and exists only near the bottom part of the reactor.

(b) the CO_2 patterns are complex reflecting oxidation in the spout and perhaps pyrolysis in the annulus.

(c) the H_2 and CO concentrations within the bed are everywhere in a molar ratio close to unity.

Gas composition profiles were not changed markedly either by char recycling (Fig. 20) or by changes in bed depth (Fig. 21) except that above the bed the H_2 and CO dropped off due to mixing of spout and annulus gas.

For the case of oxygen rather than air gasification of Forestburg coal, different types of profiles were observed (Fig. 22). At position (a) near the wall, the H_2 concentration is about twice the CO value and both level off within above 0.1 m of the orifice. At position B, the H_2/CO ratio is also about 2, and again flat until heights above the bed. In position C which should be near the center of the spout, the oxygen concentration persists at a level of about 3% all along the spout. The CO_2 level here is extremely high at about 40%, and the H_2/CO ratio remains at about 2.

Plots of annulus profiles only are shown for Balmer coal (Fig. 23). These are basically similar to those observed with Forestburg, except that the H_2/CO ratio is lower. Thus the oxygen/steam gasification profiles show

(i) H_2/CO levels are about 2 everywhere, higher than in the case of air gasification because of the higher H_2O/O_2 ratio.

(ii) profiles tend to be flatter than for air gasification and the CO_2 decreases smoothly with bed depth.

(iii)above the bed there is a drop in both H_2 and CO and a rise in CO_2 presumably due to gas phase combustion, mixing and reaction in the fountain region.

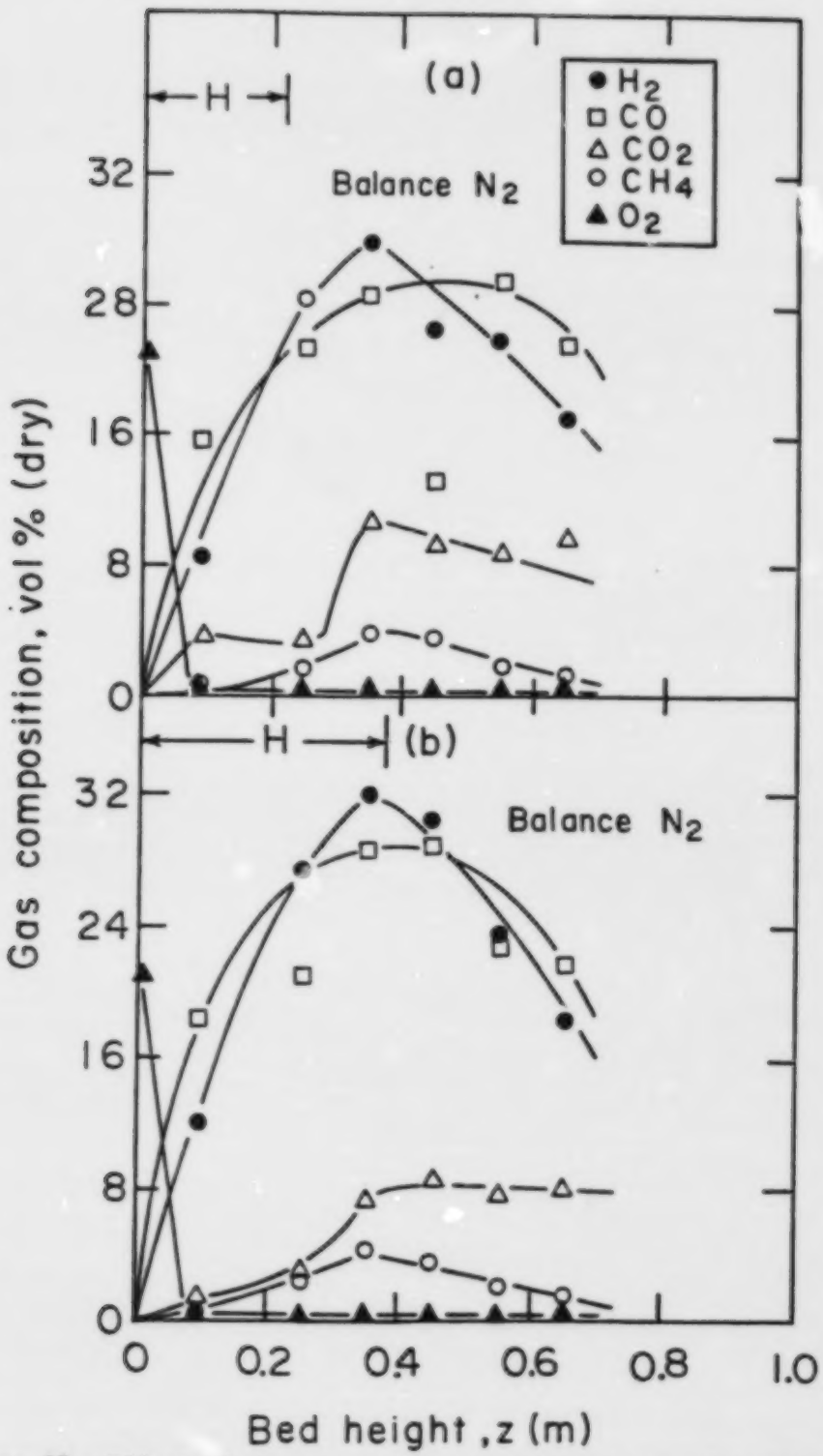

Figure 29 - Effect of char recycling on composition profiles for the Forestburg coal-air system: a) Run 90 (recycling), b) Run 62 (no recycling).

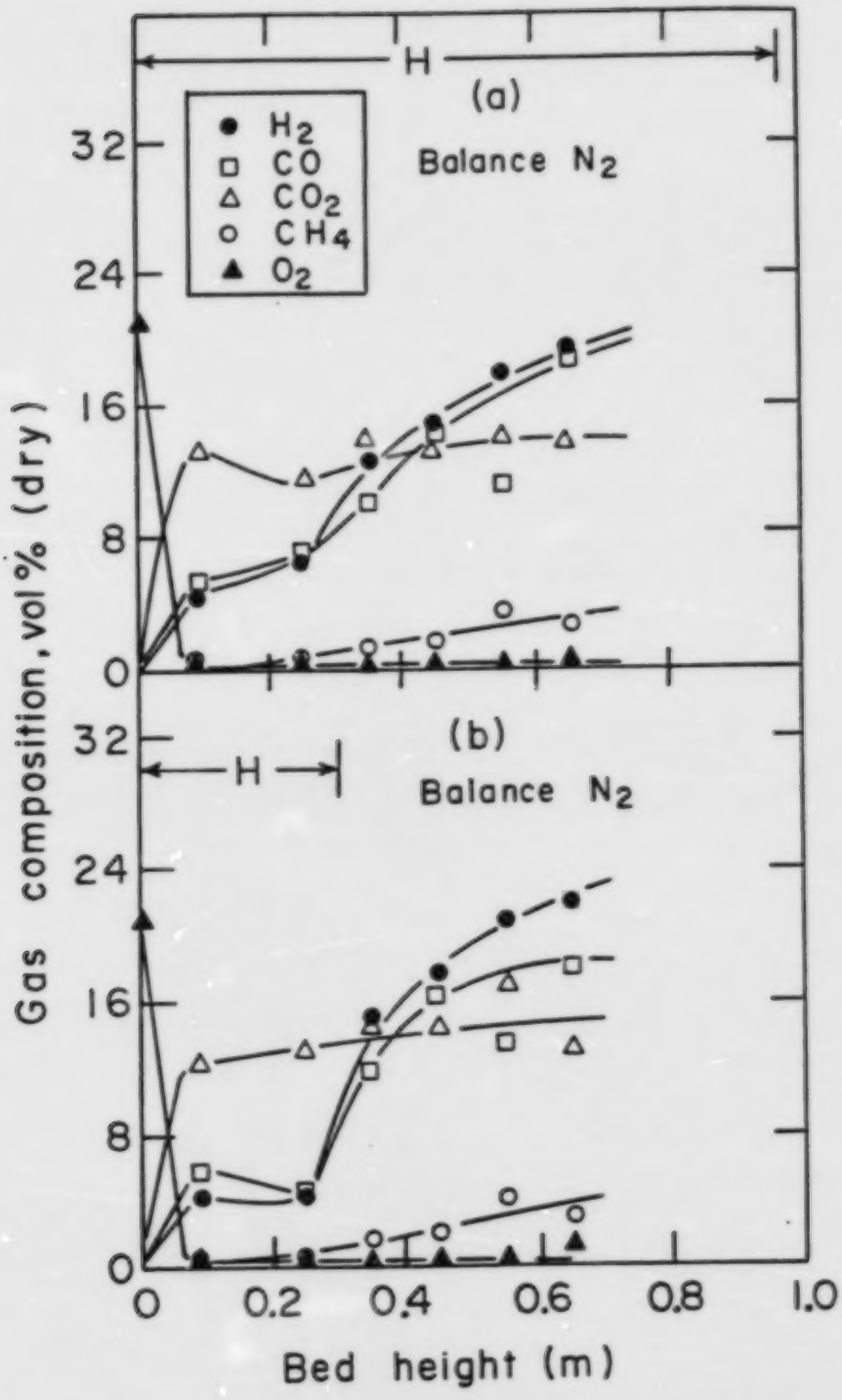

Figure 21 - Effect of the total bed height on composition profiles along position B for Forestburg coal-air system: a) Run 93, b) Run 91.

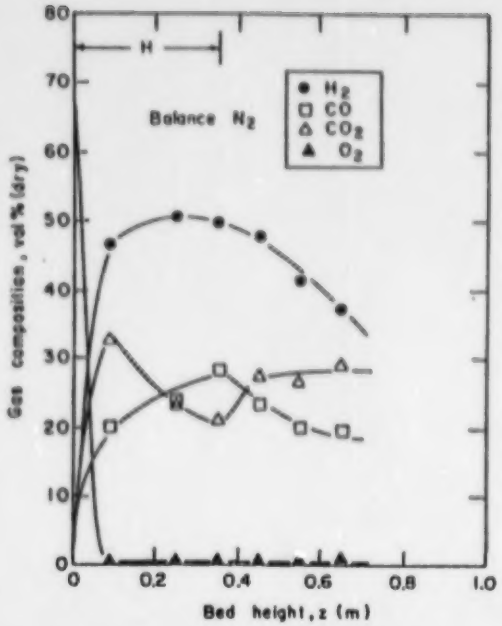

Figure 22a - Axial gas composition profiles for Forestburg coal-oxygen system along position A (Run 96).

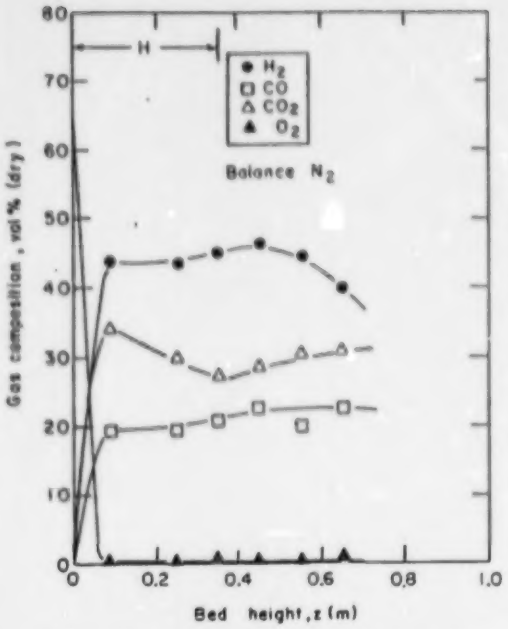

Figure 22b - Axial gas composition profiles for Forestburg coal-oxygen system along position B (Run 96).

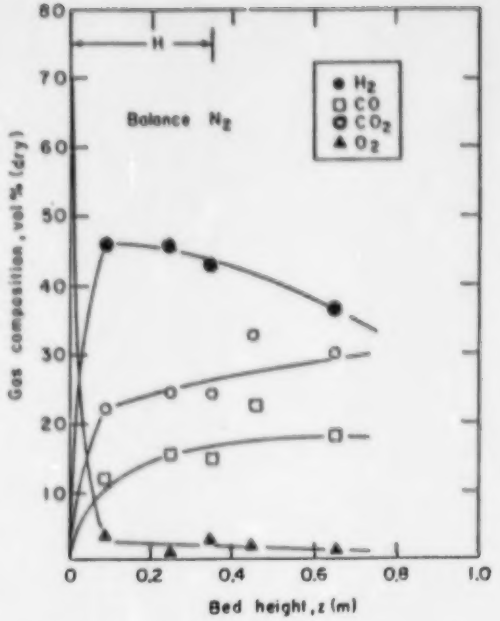

Figure 22c - Axial gas composition profiles for Forestburg coal-oxygen system along position C (Run 96).

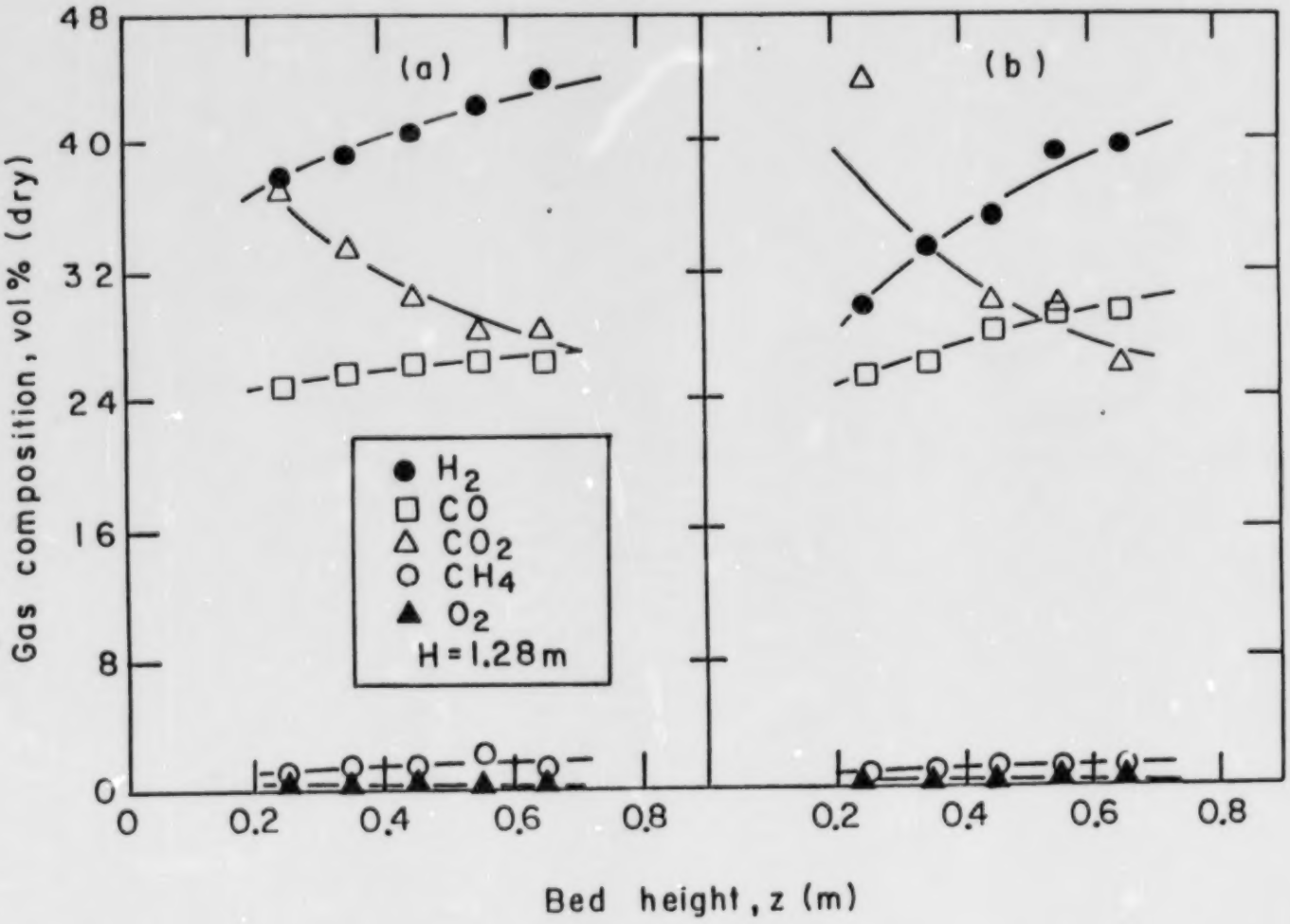

Figure 23 - Axial gas composition profiles for Balmer coal-oxygen system in Run 103: a) Along position A, b) Along position B.

Temperature profiles are shown in Figure 24-25. For air gasification of Forestburg coal (Fig. 24), there exists a large variation in the gas temperature along the spout referred to here as position C. The rapid rise from 700°C at the bed level Z = 25 cm to about 800°C at the bed level Z = 35 cm is due to combustion as evident by the rapid drop in the oxygen concentration within the same bed levels shown in Figure 19. It is the combination of combustion and low incoming gas and solid temperature that results in a very large temperature difference in the spout.

The temperature profile along position B which is close to the annulus centre is similar to that observed in a moving bed gasifier. In this case the combustion reaction is responsible for the high temperature at the bottom while the drop in temperature towards the top is due to gasification reactions.

The temperature profile along position A increases steadily to a maximum value in the lower half of the column and reduces thereafter. This low temperature at the bottom is the result of the endothermic C-H_2O and C-CO_2 reactions. The slight increase in values observed may have been due to the inflow of heat from the neighbouring region which is partly shown by the simultaneous decrease in temperatures along position B.

In addition to the axial variation in gas temperatures there is also a significant radial temperature gradient, not only between the spout and the annulus, but also within the annulus itself, especially in the lower section of the bed.

The average temperature profiles for oxygen gasification of Forestburg coal (Run 94) along positions A, B and C are plotted in Figure 25. As in the previous case the rapid increase in temperature along the spout is due to the heat released from combustion. According to Figure 22, there is still a

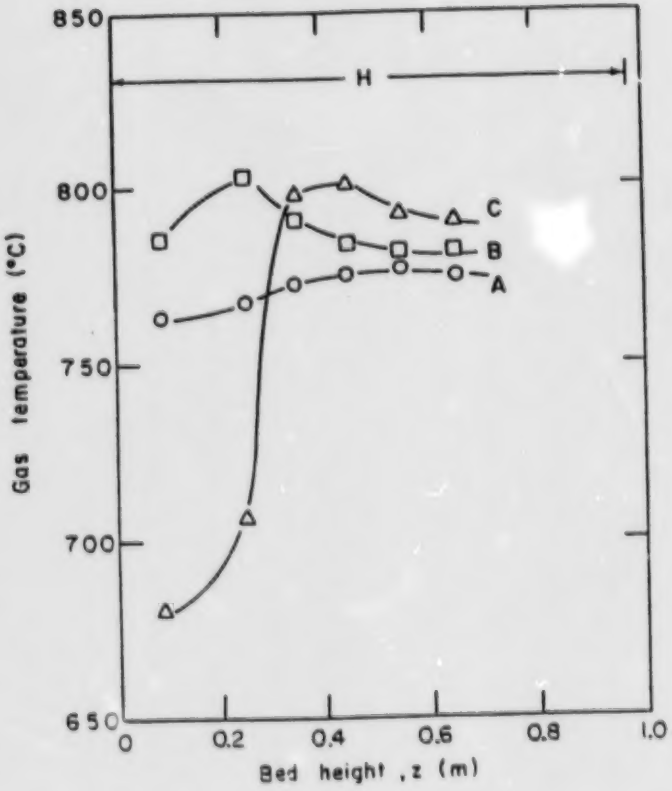

Figure 24 - Axial temperature profiles for Forestburg coal-air system (Run 93) along positions: ○ , A; □ , B; △ , C .

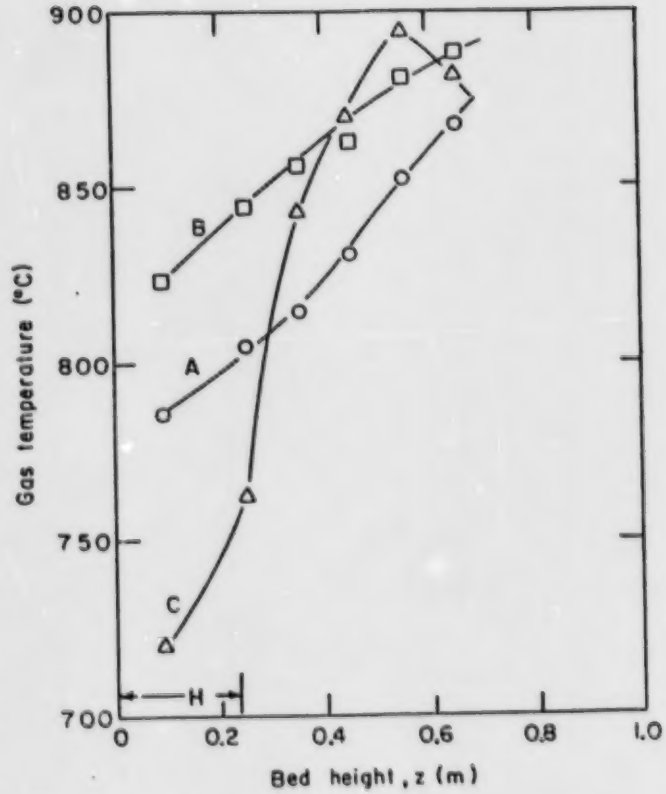

Figure 25 - Axial temperature profiles for Forestburg coal-oxygen (Run 94) along positions: ○ , A; □ , B; △ , C .

substantial amount of oxygen along the centre of the column in the fountain. Hence combustion must also be responsible for the sharp increase in the gas temperature observed along this region.

Both the temperature profiles along positions A and B show similar trends increasing throughout the bed as well as in the fountain. The steady increase in temperature in the fountain is the result of gas mixing within the region to give a higher average gas temperature than that in the annulus. A very shallow bed was employed in this run. Thus it is possible that the continuous increase in temperature along the bed in the annulus is due to the higher temperature of the incoming solids from the fountain rather than combustion. Judging from the oxygen concentration along positions A and B as shown typically in Figure 22, it is unlikely that any combustion takes place in the upper section of the bed.

9. Mathematical Model of the Spouted Bed Gasifier

This work was done by M.A.Sc. candidate Zaki Haji-Sulaiman under the primary supervision of Dr. C.J. Lim. A mathematical model of the spouted bed gasifier has been developed based on models of gas flow in the spouted bed and using the approach to the gasification problem given by Yoshida and Kunii (76) for the fluidized bed. Two-region models are used to describe the spouted bed, viz. the spout region and the annulus region. Simple plug flow in both regions may be assumed, or the more realistic stream-tube approach of Lim (4) can be used. The latter results in radial concentration differences, whereas the former predicts uniform radial concentrations. Observations show radial profiles do exist thus the more realistic stream tube model will be outlined here.

The kinetic part of the model assumes reactions 1-6 (Table 6) with reactions 1 to 3 taking place on carbon or char, and therefore coal volatiles are handled separately. Table 7 gives the simple kinetic equations which are based on the external surface area of the particle, and for which literature values are taken for the constants. The rates of gas phase reactions are taken to be instantaneous. The hydrodynamic equations for the spouted bed are given in Table 8. Plug flow of gas is assumed along the stream tubes shown in Figure 26b. Details of the mathematics of the model are summarized below. The decision of model predictions is given on p. 49.

Reactions in the Spout

A. Changes due to Gas-Solid Reactions

As an example of how the model works, consider first the spout region of constant diameter. A balance taken over an elemental height dZ leads to the following equations 8 for individual components (See Fig. 26a, and p. 52 for nomenclature).

Table 6 Reactions Assumed in Char Gasification Model

gasification:

$$C + H_2O \rightarrow CO + H_2 \qquad (6.1)$$

$$C + CO_2 \rightarrow 2CO \qquad (6.2)$$

combustion:

$$C + O_2 \rightarrow CO_2 \qquad (6.3)$$

$$CO + 1/2\ O_2 \rightarrow CO_2 \qquad (6.4)$$

$$H_2 + 1/2\ O_2 \rightarrow H_2O \qquad (6.5)$$

water gas shift:

$$CO + H_2O \rightleftharpoons CO_2 + H_2 \qquad (6.6)$$

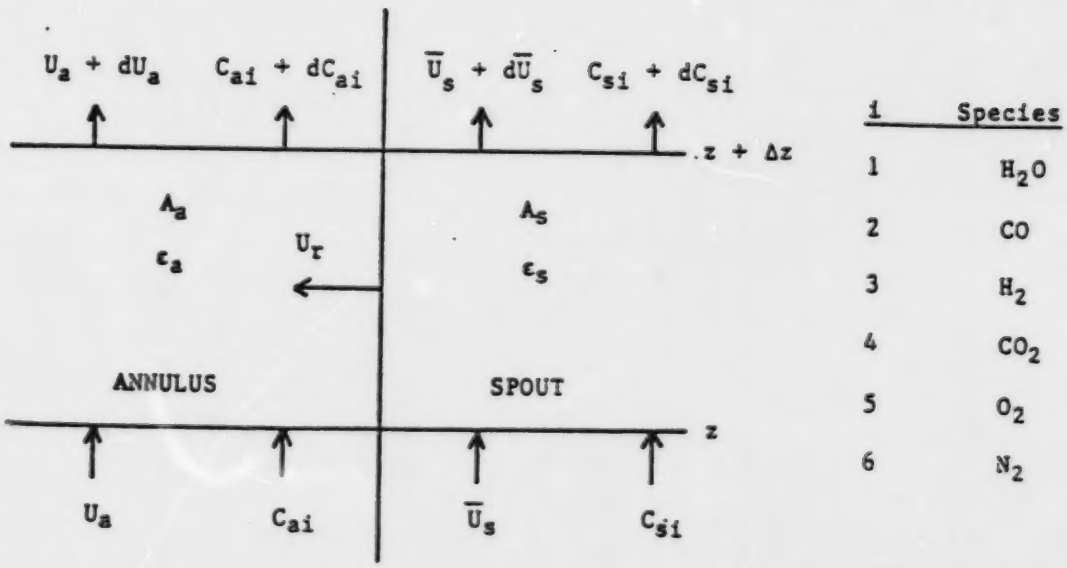

i	Species
1	H_2O
2	CO
3	H_2
4	CO_2
5	O_2
6	N_2

Fig. 26a Configuration of One Dimensional Model
(Note: Treatment of Annulus by Stream Tube Model Shown in Fig. 26b)

Table 7

Kinetic parameters used in gasification modelling

A. Reaction kinetics

$$*\text{Rate} = k_{\text{overall}_i} \exp(-E_i/RT)\ X_i^n$$

Reaction	k_{overall_i}	E_i/R	X_i	n	Unit of Rate	Ref.
Char-O_2	8710	18000	P_{O_2} (atm)	1	g/s cm^2	48
Char-CO_2	4×10^8	29790	C_{CO_2} (mol/m^3)	1	mol/m^2	30
**Char-H_2O	1.2×10^9	29790	C_{H_2O} (mol/m^3)	1	mol/m^2	

B. Equilibrium rate constant for water-gas shift reaction (63)

$$K_{ws} = 0.0265 \exp(3955/T)$$

*Based on external suface area

**Assuming rate constant of C/H_2O reaction in three times the rate constant for the C/CO_2 reaction.

Table 8

Hydrodynamic parameters for model

Parameter	Equation	Ref.
Maximum spoutable bed height	$H_m = 0.105\ d_c\ (d_c/d_p)^{0.75}\ (d_c/d_i)^{0.4}\ \lambda^2/\rho_p^{1.2}$	1
Annulus gas velocity (superficial)	$U_a = 0.88\ U_{mf}\ (1 - (1 - z/H_m)^3)$	5
Minimum spouting velocity	$U_{ms} = (d_p/d_c)\ (d_i/d_c)^{1/3} \sqrt{\frac{2g\ H(\rho_p - \rho_f)}{\rho_f}}$	1
Mean spout diameter	$D_s = 0.118\ G^{0.49}\ d_c^{0.68}/\rho_b^{0.41}$	1
Annulus voidage	$\varepsilon_a = 0.43$	
Spout voidage	$\varepsilon_s = 1 - 0.2\ \ z/H$	6
Spout gas velocity (superficial)	$\overline{U}_s = [\ U_s\ A_c - U_a(A_c - A_s)]/A_s$	
Minimum fludization velocity	$U_{mf} = 0.5\ (U_{bf} + U_{tf})$	77
Velocity beginning of fluidization	$(N_{Re})_{bf} = [(18.1)^2 + 0.0192\ N_{Ga}]^{0.5} - 18.1$	77
Velocity total fluidization	$(N_{Re})_{tf} = [(24)^2 + 0.0546\ \ N_{Ga}]^{0.5} - 24$	77

Equation and reference numbers are those of the thesis of Z. Haji-Sulaiman.

$$\bar{U}_s A_s C_{si} = [A_s \bar{U}_s + d(\bar{U}_s A_s)] [C_{si} + d C_{si}] + U_r \pi D_s C_{si} \Delta z + \sum_j R_j A_s (1 - \epsilon_s) dz \qquad (6.8)$$

where R_j, $j = 1,2,3$ are the rate of reactions represented by equations 6.1 - 6.3 respectively expressed as kmol/(m^3 of particle volume s). Ignoring any change in volumetric flux due to changes in molar flux and pressure:

$$U_r = -\frac{1}{\pi D_s} \frac{d}{dz} (\bar{U}_s A_s) \qquad (6.9)$$

Combining Equation 6.8 and 6.9 and assuming a constant spout diameter, gives the following simplified equations for individual component:

$$\frac{dC_{s1}}{dz} = \frac{-R_1(1 - \epsilon_s)}{\bar{U}_s}$$

$$\frac{dC_{s2}}{dz} = \frac{(R_1 + 2R_2)(1 - \epsilon_s)}{\bar{U}_s} \qquad (6.10)$$

$$\frac{dC_{s3}}{dz} = \frac{R_1 (1 - \epsilon_s)}{\bar{U}_s}$$

$$\frac{dC_{s4}}{dz} = \frac{(R_3 - R_2)(1 - \epsilon_s)}{\bar{U}_s}$$

$$\frac{dC_{s5}}{dz} = \frac{-R_3(1 - \epsilon_s)}{\bar{U}_s}$$

$$\frac{dC_{s6}}{dz} = 0$$

Equation 6.10 can be rewritten to give the following expression for the change in component concentration ΔC_{si} over bed height Δz resulting from gas-solid reaction

$$\Delta C_{s1} = \frac{-R_1 (1 - \epsilon_s)}{\bar{U}_s} \Delta z \qquad (6.11)$$

$$\Delta C_{s2} = \frac{(R_1 + 2R_2)(1 - \epsilon_s)}{\bar{U}_s} \Delta z \qquad (6.12)$$

$$\Delta C_{s3} = \frac{R_1 (1 - \epsilon_s)}{\bar{U}_s} \Delta z \qquad (6.13)$$

$$\Delta C_{s4} = \frac{(R_3 - R_2)(1 - \epsilon_s)}{\bar{U}_s} \Delta z \qquad (6.14)$$

$$\Delta C_{s5} = \frac{-R_3(1 - \epsilon_s)}{\bar{U}_s} \Delta z \qquad (6.15)$$

$$\Delta C_{s6} = 0 \qquad (6.16)$$

Thus the component concentration C'_{si} resulting from gas-solid reactions are given by:

$$C_{s1}' = C_{s1} + \Delta C_{s1}$$

$$C_{s2}' = C_{s2} + \Delta C_{s2}$$

$$C_{s3}' = C_{s3} + \Delta C_{s3} \qquad (6.17)$$

$$C_{s4}' = C_{s4} + \Delta C_{s4}$$

$$C_{s5}' = C_{s5} + \Delta C_{s5}$$

$$C_{s6}' = C_{s6}$$

B. Changes Due to gaseous combustion

On the assumptions that the gaseous combustion proceeds instantaneously, and as long as there is oxygen present the change in component concentrations $\Delta C'_{si}$ due to gaseous combustions is given by

$$\Delta C_{s1}' = C_{s3}'$$

$$\Delta C_{s2}' = -C_{s2}'$$

$$\Delta C_{s3}' = -C_{s3}' \qquad (6.18)$$

$$\Delta C_{s4}' = C_{s2}'$$

$$\Delta C_{s5}' = -(C_{s2}' + C_{s3}')$$

$$\Delta C_{s6}' = 0$$

Combining Equations 6.17 and 6.18 gives the component concentration $C_{si}^{"}$ after taking into consideration both the gas-solid reaction and the gaseous combustion which can be represented as follows:

$$C_{s1}^{"} = C_{s1} + \Delta C_{s1} + C_{s3} + \Delta C_{s3}$$

$$C_{s2}^{"} = 0$$

$$C_{s3}^{"} = 0 \qquad (6.19)$$

$$C_{s4}^{"} = C_{s4} + \Delta C_{s4} + C_{s2} + \Delta C_{s2}$$

$$C_{s5}^{"} = C_{s5} + \Delta C_{s5} - C_{s3} - \Delta C_{s3} - C_{s2} - \Delta C_{s2}$$

$$C_{s6}^{"} = C_{s6}$$

According to Yoshida and Kunii (76) who modelled fluidized bed coal gasification, the conversion predicted by taking into consideration gaseous combustion was very close to conversion where such reactions are neglected. The importance of considering such reactions in spouted bed char gasification modelling will be discussed later.

C. Equilibrium of Water Gas Shift Reaction

If ΔC_s is the individual change in molar concentration of H_2O, CO, H_2 and CO_2 due to water gas shift reaction, Yoshida and Kunii (76) state that the following relationship must be satisfied.

$$K_{ws} = \frac{(C_{g4}'' + \Delta C_s)(C_{g3}'' + \Delta C_s)}{(C_{g2}'' - \Delta C_s)(C_{g1}'' - \Delta C_s)}$$

$$\text{or} \qquad \Delta C_s = \frac{(K_{ws} C_{g2}'' C_{g1}'') - (C_{g4}'' C_{g3}'')}{C_{g4}'' + C_{g3}'' + K_{ws} C_{g2}'' + K_{ws} C_{g1}''} \qquad (6.20)$$

D. Equations Describing Reaction in the Spout

In the situation where C_{g2}'' and C_{g3}'' equal zero, Equation 6.20 is not applicable and the final component concentration C_{g1}''' at height $z + \Delta z$ equals C_{g1}'' represented by Equation 6.19. On the other hand if the gaseous combustion is neglected or when there is no oxygen present, the final concentration C_{g1}''' at height $z + \Delta z$ can be obtained by combining Equations 6.17 and 6.20:

$$C_{g1}''' = C_{g1} + \Delta C_{g1} - \Delta C_s$$

$$C_{g2}''' = C_{g2} + \Delta C_{g2} - \Delta C_s$$

$$C_{g3}''' = C_{g3} + \Delta C_{g3} + \Delta C_s \qquad (6.21)$$

$$C_{g4}''' = C_{g4} + \Delta C_{g4} + \Delta C_s$$

$$C_{g5}''' = C_{g5} + \Delta C_{g5}$$

$$C_{g6}''' = C_{g6}$$

E. Streamtube Model

Fig. 26 - Stream Tube Flow in the Annulus

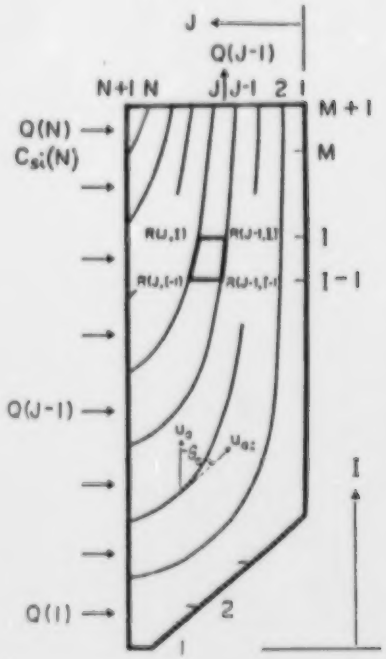

In this model as proposed by Lim and Mathur (4) vertical plug flow of gas in the spout and plug flow along curved streamlines in the annulus have been assumed. No mixing or dispersion was allowed in the

direction of flow and normal to the streamlines.

Gas Flow Path

To determine the gas flow path in the annulus, grid points were constructed by dividing the bed into N equal vertical intervals and the annulus width at the top into N equal horizontal intervals with each interval representing one flow path. Letting Q(J-1) be the volumetric flow between streamlines J-1 and J, taking overall gas mass balance at any level I gives

$$Q(J-1) = U_a(I)*[R(J-1, I)^2 - R(J,I)^2] \qquad (6.30)$$

where $U_a(I)$ is the superficial annulus gas velocity at level I and R(J,I) specifies the ordinate of the streamline J at level I (the column axis is taken as the reference). The first streamline (J=1) was assumed to coincide with the column wall. Letting the interval between streamlines J and J+1 be the flow path J, the superficial gas velocity $U_{az}(I)$ along flow path J was calculated using the relationship.

$$U_{az}(I) = U_a(I)/\text{Cos}\ \theta_a \qquad (6.31)$$

In this model θ_a was taken to be the angle formed between the line joining the centre of flow path J at levels I and I-1 and the horizontal. Denoting PL(I) as the distance between these two centre points, the total path length for flow path J from the spout-annulus interface to the top of the bed at I=N was given by $\sum_{I} PL(I)$.

Reactions in the Annulus

A. Changes Due to Gas-Solid Reactions

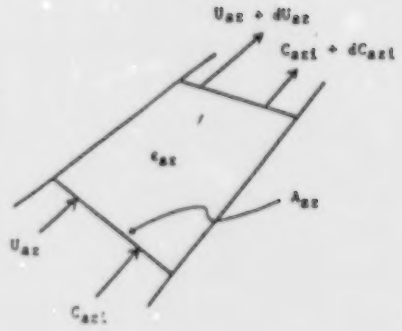

A component mass balance over length dL along the flow path J gives

$$U_{az}A_{az}C_{azi} = [A_{az}U_{az} + d(A_{az}U_{az})][C_{azi} + dC_{azi}] + \sum_j R_j A_{az}(1 - \epsilon_{az})\, dL \qquad (6.32)$$

On the assumption of no change in volumetric flow due to the change in molar flow and pressure, Equation 6.32 reduces to the following expressions for the change in the individual component concentration ΔC_{azi} over the path lengh ΔL due to the gas-solid reactions:

$$\Delta C_{az1} = \frac{-R_1(1 - \epsilon_{az})}{U_{az}} \Delta L \qquad (6.33)$$

$$\Delta C_{az2} = \frac{(R_1 + 2R_2)(1 - \epsilon_{az})}{U_{az}} \Delta L \qquad (6.34)$$

$$\Delta C_{az3} = \frac{R_1(1 - \epsilon_{az})}{U_{az}} \Delta L \qquad (6.35)$$

$$\Delta C_{az4} = \frac{(R_3 - R_2)(1 - \epsilon_{az})}{U_{az}} \Delta L \qquad (6.36)$$

$$\Delta C_{az5} = \frac{-R_3(1 - \epsilon_{az})}{U_{az}} \Delta L \qquad (6.37)$$

$$\Delta C_{az6} = 0 \qquad (6.38)$$

In this case $\epsilon_{az} = \epsilon_s$.

B. Changes Due to Gaseous Combustion and Water Gas Shift Equilibrium

Following the same procedure adopted in all the previous cases, the expressions for ΔC_{az} due to the water gas shift equilibrium and the final component concentrations at the path length L + ΔL were derived and were in the same form given by Equations 6.18 - 6.20 but at conditions referring to those in the flow path J.

Outlet Component Gas Concentration

The final component gas concentration leaving the gasifier was calculated by combining the streams leaving each region. Thus the exit gas concentration C_{ei} for component i can be expressed as

One-dimensional model:

$$C_{ei} = \frac{U_{aH} A_a C_{aHi} + \bar{U}_{aH} A_a C_{aHi}}{U_g A_c} \qquad (6.39)$$

Streamtube model:

$$C_{ei} = \frac{\left[\sum_{j=1}^{N-1} U_{aH} A_{aHj} C_{aHi(j)}\right] + \bar{U}_{aH} A_a C_{aHi}}{U_g A_c} \qquad (6.40)$$

Any reaction in the fountain has been ignored.

Calculation Procedure

The equations describing the change in gas concentration due to the gas solid reactions given by Equations 6.10 - 6.15 for the spout, and Equations 6.33 - 6.37 for the flow path J in the streamtube model are non-linear differential equations and were solved using the 4th order Runge-Kutta technique.

For the streamtube model, the gas concentration profiles in the spout were initially obtained using the inlet gas concentration as the boundary conditions. The gas concentrations along the gas flow path J were then solved using the gas concentration in the spout taken at the mid point between streamlines J and the J + 1 as the inlet condition.

Model Simulation and Discussion

A number of simulated runs were performed using both the one-dimensional and the streamtube models to predict the axial and the radial gas composition profiles as well as the overall conversion achieved from a spouted bed coal gasifier. The column geometry used in the experimental system has been chosen for this purpose, using air/oxygen and steam as the only gasification medium. In addition, the importance of some operating variables such as the total bed height and the bed temperature in determining the gasifier performance was also investigated.

Model Results and Comparison to Measured Values

Figures 27 and 28 show predicted axial gas composition profiles for the annulus for both models. Figure 29 shows the corresponding plot for the spout. In the annulus the predicted oxygen concentration immediately drops to zero, whereas its predicted value in the spout drops off slowly with height. This latter feature is not present in the experimental measurements. The kink in the annular profiles is due to the change in geometry at the cone/cylinder junction of the spouted bed. The radial profile predicted at the top of the spouted bed is shown in Fig. 30. Again the oxygen breakthrough is predicted. Figure 31 shows predicted and measured axial profiles. The model predictions can be said to show reasonable trends with experimental data, and indeed are very close given the weaknesses of the model. It should be borne in mind that kinetic expressions are taken from the literature, and are not for the particular coals tested. A much better fit to the data would be expected if some valid single particle kinetic data were available for the coals used. The problem of the volatile release is discussed at length in the thesis of Z. Haji-Sulaiman. It is important to note that the current model kinetics is for chars, and the volatiles have been added in to the exit gas in these calculations. The model also assumes isothermal conditions throughout the reactor, whereas experiment show this to be untrue. Finally no account is taken of particle velocities in the model. As the model is developed further improvements in prediction can be expected.

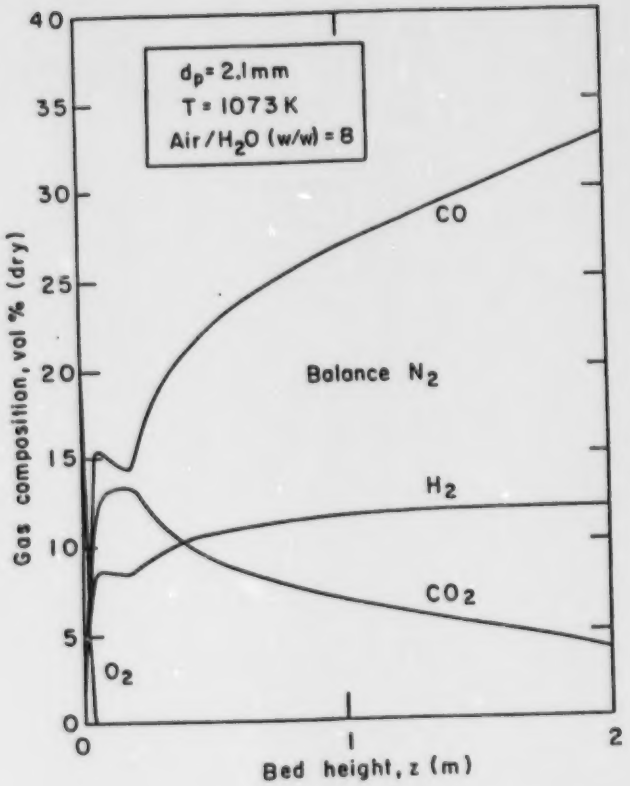

Figure 27 - Axial gas composition profiles in the annulus predicted using the one-dimensional model.

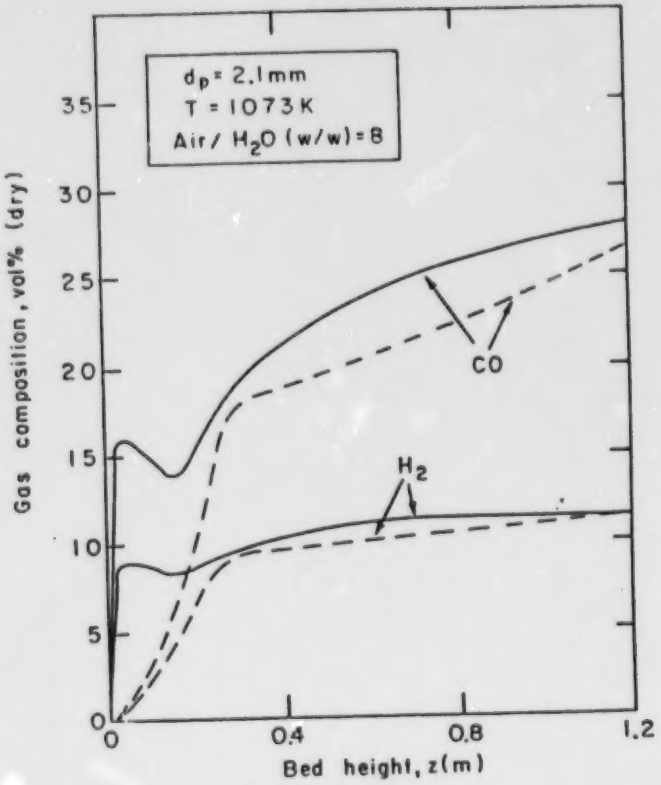

Figure 28 - Comparison on the axial hydrogen and carbon monoxide profiles along the centre of annulus; —— , one-dimensional model; - - -, streamtube model.

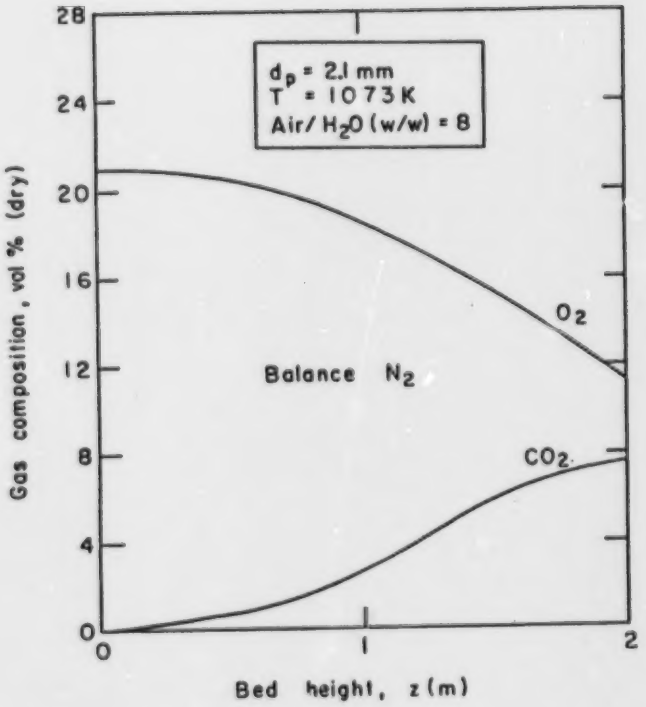

Figure 29 - Axial gas composition profiles in the spout predicted using the one-dimensional model.

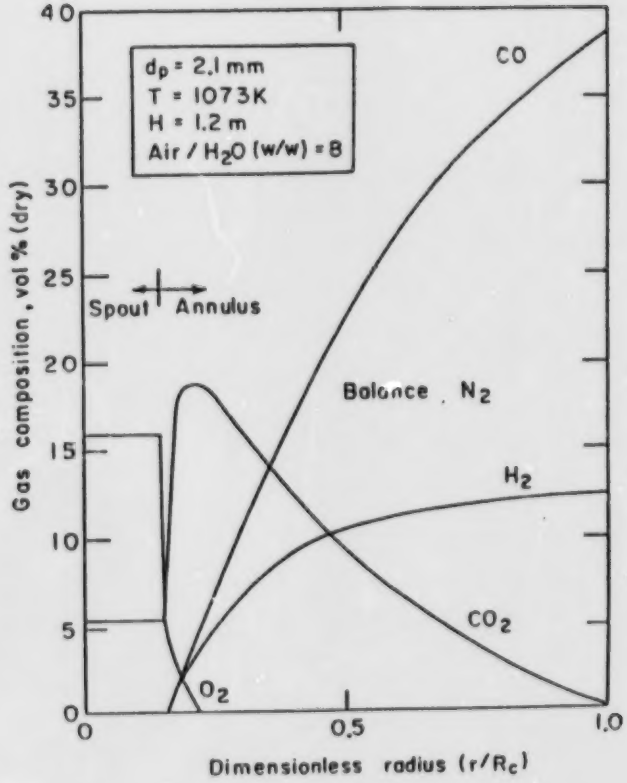

Figure 30 - Radial gas composition profiles at the top of the bed predicted using the streamtube model.

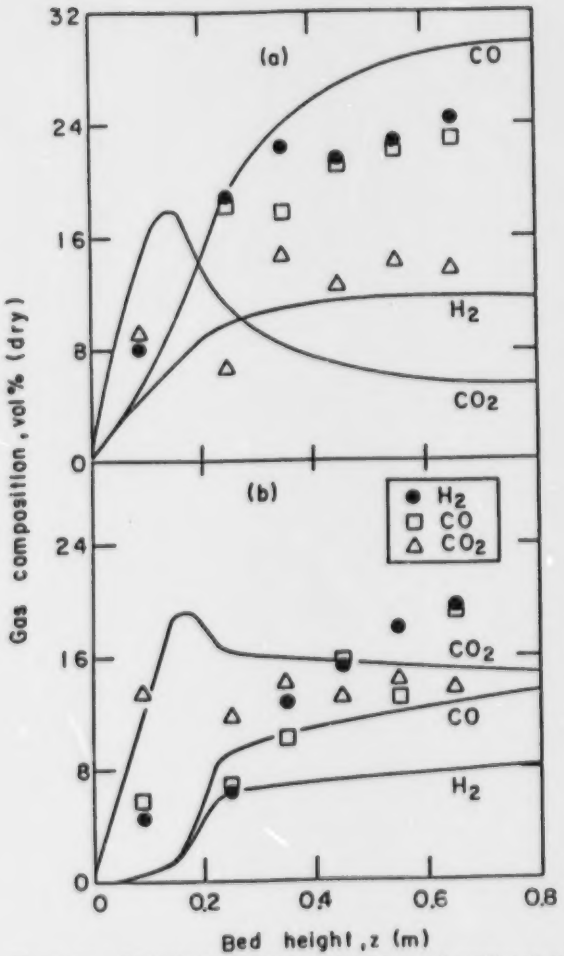

Figure 31 - Comparison between experimental and predicted axial profiles using the one-dimensional model: a) Along position A, b) Along position B.

NOMENCLATURE

A_a	cross-sectional area of annulus, m^2
A_c	cross-sectional area of column, m^2
A_p	surface area of a single particle, m^2
A_s	cross-sectional area of spout, m^2
C_{ai}	concentration of component i in annulus gas, mol/m^3
C_{aiH}	C_{ai} at z = H, mol/m^3
C_{azi}	concentration of component i along streamline in streamtube model, mol/m^3
C_{aziH}	C_{azi} at z = H, mol/m^3
C_{ei}	concentration of component i leaving reactor, mol/m^3
C_g	gas concentration, mol/cm^3 unless otherwise specified
C_s	carbon concentration of char; C_{so}, same at zero conversion, mol/cm^3 unless otherwise specified
C_{si}	concentration of component i in spout gas, mol/m^3
C_{siH}	C_{si} at z = H, mol/m^3
Cp	specific heat capacity, J/kg:K
D	diffusion coefficient; D', same for oxygen, cm^2/s
D_e	effective diffusivity in solid; D_{eo}, same at zero conversion, cm^2/s
d_c	column diameter, m
d_i	gas inlet diameter, m
d_p	particle diameter, m unless otherwise specified
d_s	spout diameter, m

E'	activation energy for pyrolysis, kJ/mol
E	activation energy for char-gas reaction, kJ/mol
F_w	a parameter used in Equation 2.34
f_1, f_o	relative reactivity factor for char-H_2O reaction used for Johnson kinetics (Eqn. 2.22)
G	gas mass flow rate per unit of column cross-section, $kg/m^2.s$
Ga	Galileo number
g	acceleration of gravity ($9.81\ m/s^2$)
H	bed depth, unexpanded, m
H_m	maximum spoutable bed depth, m
h	heat transfer coefficient, $W/m^2.°K$
K	equilibrium constant for char-gas reaction
K_{ws}	equilibrium constant for water gas shift reaction
k', k'_o	pyrolysis rate constant, s^{-1}
k_1, k_2, k_3	constants of Langmuir-Hinshelwood type rate expressions for char-CO_2 and char-H_2O reaction
k_I	rate constant for char-H_2O reaction in Johnson kinetic (Eqn. 2.22)
k_{ash}	ash film diffusion rate constant, $g/cm^2.atm.s$
k_c	thermal conductivity of coal, $W/m.°K$ m
k_{diff}	diffusional reaction rate constant for char-gas reaction, $g/cm^2.atm.s$
$k_{overall}$	overall rate constant for char-gas reaction as defined by Equation 6.7, $g/cm^2.atm.s$
k_s, k_{so}	surface reaction rate constant for char-gas reaction $g/cm^2.atm.s$
k_v, k_{vo}	volumetric rate constant for char-gas reaction $(cm^3/mol)^n.s^{-1}$
L	latent heat of vapourisation of water, J/kg
MC	coal moisture content, fraction, dry basis; MC_o, same at zero time
M_w	molecular weight of carbon, g/mol
m_p	mass of a single particle, kg/m^3
Nu	Nusselt number
n	order of reaction with respect to gaseous reactant concentration or partial pressure
P	total pressure, atm
P_1, P_2, P_3	Reactants partial pressure in Langmuir type rate equation, atm
P_g	gas partial pressure, atm
PL	path length along streamline, m
Pr	Prandalt number
Q_o	inlet gas flowrate, kg/h
Q(J-1)	volumetric gas flow along streamline J, m^3/s
R	universal gas constant (8.314 J/mol.°K)
R'	universal gas constant (82.06 $atm.cm^3/mol.°K$)
R_c	column radius, m
Re	Reynolds number
$(Re)_{bf}$	Reynolds number at beginning of fluidization
$(Re)_{tf}$	Reynolds number at complete fluidization
R_j	rate of jth reaction given by equation 6.1 - 6.3, $kmol/m^3$ of particle volume.s

r_c	core radius at time t in the core shrinking model; r_o, same at t = 0, m unless otherwise specified
r	radial distance from the column axis, m unless otherwise specified
Sc	Schmidt number
T	temperature, °K
T_o	maximum temperature to which char has been exposed prior to gasification, °K
T_{wb}	adiabatic wet bulb temperature, °K
t	time, s
U_a	superficial gas velocity in annulus, m/s
U_{aH}	U_a at z=H, m/s
U_{az}	superficial gas velocity along streamline, m/s
U_{bf}	superficial gas velocity at beginning of fluidization m/s
U_{mf}	minimum fluidization velocity, m/s
U_{ms}	minimum spouting velocity, m/s
U_r	radial gas cross flow velocity at spout-annulus interface, m/s
U_s	gas spouting velocity, m/s
$\bar{U}_s$	superficial gas velocity in spout, m/s
U_{tf}	superficial velocity at complete fluidization, m/s
u_s	gas sampling velocity; u_{iso}, same at isokinetic condition, m/s
V	volatiles loss from particle up to time t, fraction of original coal weight
X_{vm}	proximate volatile matter content of coal, gm/gm of coal (daf)
x	fraction of carbon conversion of char due to char-gas reaction
Y	r_c/r_o.
z	vertical distance from gas inlet, m unless otherwise specified

Greek Symbols

α	a parameter in Johnson kinetic, equation 2.22
α_v	relative pore surface area function in volumetric reaction model
ε	voidage of the ash layer
ε_a	annulus voidage
ε_{az}	voidage along streamline
ε_s	spout voidage
ρ_b	solid bulk density, kg/m^3 except for calculating D_s (Table 9) where it should be expressed in g/cm^3
ρ_c	molar density of carbon in coal particle, mol/cm^3
ρ_f	gas density, kg/m^3
ρ_p	particle density, kg/m^3 except for calculating H_m (Table 9) where it should be expressed in g/cm^3
ρ_{ar}	raw coal density, kg/m^3
η	effectiveness factor
ψ	product distribution of char combustion defined by Equation 2.17
λ	shape factor of particle. $\lambda = 1$ for spherical particle

10. Conclusions and Further Work

The experimental and computational work carried out over the past 13 months has shown:

1. The spouted bed gasifier can be efficiently operated in the char-bed dry-ash mode with air and with oxygen as oxidant on bituminous and sub-bituminous coals. Gas heating values of 9.6 MJ/m^3 have been obtained with oxygen/steam gasification.
2. Suitable geometry and flow conditions have been found to operate in the agglomerating ash mode. In the best run spherical agglomerates of about 5-mm dia. and < 1% wt. carbon were produced.
3. Catalytic gasification with K_2CO_3 appears to raise efficiency, and reduce H_2S levels in the produced gas. Some problems were experienced with the hygroscopic nature of the treated coal.
4. Sulphur levels in the produced gases represent roughly 30-40% of the sulphur in the incoming coal with 95% present as H_2S.
5. In-bed measured profiles of concentration and temperature have defined the combustion zone for both air and oxygen gasification. Profiles have been established for a wide range of conditions.
6. A kinetic model of the spouted bed gasifier has been developed to predict axial and radial composition profiles in the gasifier. Using literature kinetic data, gives reasonable predictions, but features of experimental measurements are not reproduced.

Further work is required to develop continuous removal of agglomerated ash. The conditions for optimal operation and control of agglomerate size have not been established. Catalytic effects have just been touched - the role of salt loading, and comparison with non-catalytic gasification at similar particle size have not been explored. The mathematical model of the

process should be run with kinetic data specific to the coals tested in order to have reasonable expectations of success. As a less-desireable alternative, the model could be inverted to yield kinetic coefficients from experimental profiles. However some stability problems are foreseen, and the appropriateness of the model particularly for scale-up could not be firmly established.

REFERENCES

Sections 1 to 8

1. Watkinson, A.P., S.K. Foong, C.B. Prakash and G. Cheng, "Spouted Bed Gasification of Western Canadian Coals", CANMET Contact Report OSU80-00068 (1981).

2. Watkinson, A.P, C.B. Prakash, G. Cheng and S. Low, "Spouted Bed Gasification of Western Canadian Coals", CANMET Contract Report OSU81-00074 (1982).

3. Watkinson, A.P., G. Cheng and S. Low, "The Continued Study of Spouted Bed Gasification of Western Canadian Coal", CANMET Contract Report OSU82-00138 (1983).

4. Watkinson, A.P., G. Cheng and C.B. Prakash, "Comparison of Coal Gasification in Fluidize and Spouted Beds", Can. J. Chem. Eng. 61, 468-474 (1983).

Section 9

1. Mathur, K.B. and Epstein, N., "Spouted Beds", Academic Press, New York (1974).

4. Lim, C.J. and Mathur, K.B., AIChEJ 22, 674 (1976).

5. Piccinini, N., Grace, J.R., and Mathur, K.B., Chem. Eng. Sci. 34. 1257 (1979).

6. Littman, H, Narayanan, P.V., Tomlins, A.H. and Friedman, M.L, AIChE Sym. Ser. No. 205, 77, 174 (1981).

30. Dutta, S. and Wen, C.Y. I.E.C. Proc. Des. Dev. 16, 20 (1977).

48. Field, M.A., Gill, D.W., Morgan, B.B. and Hawksley, P.G.W., "Combustion of Pulverized Coal", BCURA, Leatherhead (1967).

76. Yoshida, K. and Kunii, D.
JChE Japan 7, 34-9 (1974).

77. Vaid, R.P. and Sen Gupta, P.
Can. J. Ch.E. 56, 292 (1978).

APPENDIX A

Table A-1 Run Conditions and Results (All Runs 1983-4)

RUN NO	COAL	COAL % H_2O	COAL dp (mm)	GAS'N MODE	FEEDRATE* (kg/h) m_a	m_c	m_A	m_s	m_{ch}	m_{ox}/m_{ox}	m_s/m_c	TEMP °C AVG	TEMP °C MAX	G.H.V. MJ/m³	GAS YIELD m³/kg	GAS ANALYSIS (% MOL) H_2	CO	CO_2	CH_4	N_2	% C CONVERSN	CYCLONE CATCH kg/h	CYCLONE CATCH % C	η_{HOT} (%)	% H_2O DECOMP	RUN DURATN hr:min
86	BALMER	1.47	2.00	SP		46.46	99.34	5.84	—	0.498	0.126	819	870	3.49	2.16	12.02	8.77	14.18	2.47	62.55	31.10	26.10	82.97	28.90	36.74	3:00
87	BALMER	1.47	2.00	SP		TEST		RUN	FOR	THE	IN-	BED	GAS	SAMPL	ING	PROBE										2:29
88	FORESTBURG	23.71	2.06	SP		25.17	92.54	9.53	—	0.856	0.379	770	798	3.60	3.93	13.63	11.89	14.37	1.94	58.17	76.38	15.39	81.30	69.43	50.14	2:55
89	FORESTBURG	23.71	2.06	SP		27.80	113.30	10.53	—	0.949	0.379	862	893	3.76	4.38	12.56	14.04	12.93	1.44	59.02	83.91	11.49	71.27	76.81	54.04	3:34
90A	FORESTBURG	23.71	2.06	SP		27.43	107.38	10.38	4.17	0.791	0.378	831	872	3.62	4.20	12.63	14.88	13.15	1.27	58.07	79.10	4.97	72.34	76.07	53.23	7:01
90B	FORESTBURG	23.71	2.06	SP		27.43	104.96	10.38	—	0.891	0.378	915	936	3.71	4.13	12.39	15.33	12.69	0.94	58.64	79.67	4.97	72.34	73.19	50.13	7:01
91	FORESTBURG	23.71	2.06	SP		31.56	100.51	11.95	2.74	0.682	0.379	795	818	4.14	3.67	15.02	13.83	14.29	1.74	55.13	73.96	7.25	76.82	66.70	52.83	6:00
92	FORESTBURG	23.71	2.06	SP		28.93	104.22	10.95	2.55	0.771	0.379	791	836	3.78	3.98	12.80	13.51	14.95	1.59	57.14	80.61	5.90	79.81	68.84	49.81	2:46
93	FORESTBURG	23.71	2.06	SP		34.94	102.98	13.23	2.96	0.633	0.379	774	817	3.95	3.31	14.53	12.27	14.85	1.87	56.48	64.64	8.51	82.91	59.24	47.02	5:09
94	FORESTBURG	23.71	2.06	SP	32.21	29.79		27.11	—	1.081	4.27	901	975	7.49	1.67	36.90	18.02	41.98	2.21	0.89	69.96	6.40	68.00	79.99	10.09	6:01
95	FORESTBURG	23.71	2.06	SP	25.07	32.68		8.38	2.90	0.705	2.58	731	746	7.19	2.09	35.32	12.69	36.84	3.63	11.52	74.65	4.15	81.17	72.30	19.05	2:36
96A	FORESTBURG	23.71	1.40	SP	25.00	37.57		6.23	—	0.665	2.30	738	744	6.32	1.98	36.48	14.85	38.23	0.28	10.16	71.21	7.97	72.35	60.63	20.45	4:15
96B	FORESTBURG	23.71	1.40	SP	26.06	30.05		5.38	—	0.867	2.84	804	850	6.96	1.71	35.91	21.59	33.74	0.00	8.76	63.76	7.97	72.35	64.47	14.52	4:15
97C	FORESTBURG	23.71	1.40	SP	27.18	29.68		5.23	—	0.916	2.198	857.5	996	9.23	1.02	37.75	30.52	28.72	2.56	0.45	42.41	14.80	70.91	53.86	11.29	1:55
98	FORESTBURG	23.71	1.40	SP	27.18	34.94		7.23	—	0.778	1.924	863.8	900	9.14	1.68	36.76	27.37	32.08	3.65	0.14	71.57	6.57	77.60	72.26	20.33	2:11
99	FORESTBURG	23.71	1.40	SP	27.16	30.99		1.73	—	0.876	2.315	844.2	895	8.38	1.83	38.32	24.47	34.80	2.07	0.33	75.53	4.30	77.34	74.71	19.70	3:47
100	FORESTBURG	23.71	1.40	SP	26.10	33.44		2.67	—	0.781	2.173	805.0	818	8.79	1.81	39.14	22.02	34.95	3.65	0.24	73.95	5.71	72.93	74.08	21.01	2:08
101	BALMER	1.30	1.59	SP	25.46	44.54		6.66	—	0.572	2.170	813.3	873	9.09	0.92	32.43	31.03	32.53	3.74	0.27	35.15	26.46	87.99	36.60	8.75	2:56

* m_c COAL, MAF BASIS; η_{HOT} = HOT GAS EFFICIENCY; SP = SPOUTED BED $m_{ox} = m_{O_2} + .23 m_A$ m_{O_2} = PURE OXYGEN $m_{ch} = m_c + m_{ch}$ m_{ch} = CHAR, MAF BASIS

Table A-1 Cont'd

RUN NO	COAL	COAL % H_2O	COAL dp (mm)	GAS'N MODE	FEEDRATE * (kg/h) m_a	m_c	m_A	m_s	m_{ch}	m_{ox}/m_{O_2}	m_s/m_c	TEMP °C AVG	MAX	G.H.V. MJ/m^3	GAS YIELD m^3/kg	GAS ANALYSIS (% mol) H_2	CO	CO_2	CH_4	N_2	% C CONVERSN	CYCLONE CATCH kg/h	% C	η_{HOT} (%)	% H_2O DECOMP	RUN DURAT'N hr:min
102	BALMER	1.30	1.59	sp	26.91	27.25		73.91	—	0.988	2.712	871.3	894	8.88	0.77	34.93	22.42	37.26	5.12	0.17	28.43	21.12	82.23	33.69	6.55	1:38
103	BALMER	1.30	1.59	sp	26.35	32.48		72.49	—	0.811	2.231	897.8	927	9.48	1.52	36.95	29.77	29.58	3.71	0.00	54.69	16.29	80.20	57.25	16.10	2:43
104	BALMER	1.30	1.59	sp	26.14	24.63		72.37	—	1.061	2.938	921.8	937	9.03	1.64	35.29	30.73	30.98	2.76	0.23	60.27	11.54	75.25	63.97	13.10	2:06
105	BALMER	1.30	1.59	sp	25.36	24.63		72.37	—	1.030	2.938	984.2	1013	9.16	1.79	36.76	31.95	28.75	2.26	0.30	64.42	10.65	73.28	70.32	14.94	5:16
106	Pulverized CHAR	12.70	2.06	sp	23.27	—		15.18	25.12	0.926	0.604	901.6	955	2.945	4.045	10.64	12.63	14.34	0.36	62.04	70.63	13.08	79.81	59.92	33.95	3:26
107	BALMER	1.30	1.59	sp	29.57	28.61		72.42	—	1.034	2.531	1094	1141	8.71	1.94	35.16	33.58	29.84	1.06	0.37	71.42	10.01	72.72	71.87	17.57	2:51
108	BALMER	1.30	1.59	sp	29.92	30.92		72.47	—	0.968	2.344	1003.9	1017	9.05	1.89	37.08	33.85	27.50	1.25	0.33	67.57	12.09	74.53	68.85	19.22	3:09
109	BALMER	4.03	1.59	sp	25.02	19.30		77.93	—	1.297	4.038	971.8	1027	8.77	2.25	36.92	28.85	31.76	2.15	0.32	80.76	6.24	52.98	87.15	14.20	2:41
110	BALMER	2.05	1.59	sp	25.21	16.14		75.37	—	1.562	4.670	971.1	980	9.02	1.645	39.32	29.03	29.62	1.98	0.06	56.95	6.75	56.10	76.44	9.66	2:56
111	BALMER	2.05	1.59	sp	24.92	20.35		82.67	2.056	1.112	4.062	924.6	959	8.036	2.27	34.80	25.45	28.33	1.98	9.44	72.36	7.94	63.08	81.69	13.43	3:55
112	BALMER	1.30	1.59	sp	29.30	26.93		68.04	—	1.088	2.526	1124.4	1183	8.594	2.21	36.00	31.60	31.01	1.11	0.29	80.57	7.58	61.62	81.23	18.55	3:00

* m_c COAL, MAF BASIS; η_{HOT} = HOT GAS EFFICIENCY; sp = SPOUTED BED $m_{ox} = m_{O_2} + .23 m_A$ m_{O_2} = PURE OXYGEN $m_{cx} = m_c + m_{ch}$ m_{ch} = CHAR, MAF BASIS

Table A-2 Forestburg Coal Runs - Summary of Results

RUN No	FEED RATE *(kg/kg)					(°C)		G.H.V.	G.Y.	m_{ox}/m_{cx}	GAS ANALYSIS (DRY BASIS)					% C	G.N.V.	G.Y./	m_s/m_c	INIT. BED WT	FINAL BED WT	GAIN/LOSS IN BED WT
	m_c	m_{o_2}	m_a	m_s	m_{ch}	$\bar{T}_b$	T_{max}	mJ/m^3	m^3/kg	(kg/kg)	H_2	CO	CO_2	CH_4	N_2	CONVERN	* m_c	m^3/kg		(kg)	(kg)	(kg)
88	25.17		92.54	9.53	—	770	798	3.60	3.93	0.856	13.63	11.89	14.37	1.94	58.17	76.38	90.61	1.56×10^{-1}	0.379	19.08	22.73	3.65
89	27.80		113.30	10.53	—	862	893	3.76	4.38	0.949	12.56	14.04	12.93	1.44	59.02	83.91	104.53	1.58×10^{-1}	0.379	19.20	9.09	-10.11
90B	27.43		104.96	10.38	—	915	936	3.71	4.13	0.891	12.39	15.33	12.69	0.94	58.64	79.67	101.77	1.51×10^{-1}	0.378	18.51	5.68	-12.83
94	29.79	32.21		127.11	—	901	975	7.49	1.67	1.081	36.90	18.02	41.98	2.21	0.89	69.96	223.13	5.64×10^{-2}	4.27	22.73	3.86	-18.87
96A	37.57	25.00		86.23	—	738	744	6.32	1.98	0.665	36.48	14.85	38.23	0.28	10.16	71.21	237.44	5.27×10^{-2}	2.30	22.73	8.30	-14.43
96B	30.05	26.06		85.38	—	804	850	6.96	1.71	0.867	35.91	21.59	33.74	0.00	8.76	63.76	209.15	5.69×10^{-2}	2.84	22.73	8.30	-14.43
** 106		23.27		15.18	25.12	901.6	955	2.945	4.045	0.926	10.64	12.63	14.34	0.36	62.04	70.63	73.99	1.61×10^{-2}	0.604	20.45	9.89	-10.56
90A	27.43		107.38	10.38	4.17	831	872	3.62	4.20	0.791	12.63	14.88	13.15	1.27	58.09	79.10	99.30	1.53×10^{-1}	0.378	18.51	5.68	-12.83
91	31.56		100.51	11.95	2.74	795	818	4.14	3.67	0.682	15.02	13.83	14.29	1.74	55.13	73.86	130.66	1.16×10^{-1}	0.379	17.62	6.70	-10.92
92	28.93		104.22	10.95	2.55	791	836	3.78	3.98	0.771	12.80	13.51	14.95	1.59	57.14	80.61	109.36	1.38×10^{-1}	0.379	22.46	26.02	3.56
93	34.94		102.98	13.23	2.96	794	817	3.95	3.31	0.633	14.53	12.27	14.85	1.87	56.48	64.64	138.01	9.47×10^{-2}	0.379	22.73	32.56	9.83
95	32.68	25.07		84.38	2.90	731	746	7.19	2.09	0.705	35.32	12.69	26.84	2.63	11.52	74.65	234.97	6.40×10^{-2}	2.58	19.28	24.66	5.38

RUN 88, 89, 90B, 94, 96A, 96B, 106 FORESTBURG COAL GASIFICATION RUN WITHOUT DUST RECYCLING
RUN 90A, 91, 92, 93, 95 FORESTBURG COAL GASIFICATION RUN WITH DUST RECYCLING

** ALL m_c VALUES IN RUN 106 ARE IN TERMS OF m_{ch} VALUES

* m_c COAL, MAF BASIS; $m_{ox} = m_{o_2} + .23 m_a$ m_{o_2} = PURE OXYGEN $m_{cx} = m_c + m_{ch}$ m_{ch} = CHAR, MAF BASIS

Table A-3 Balmer Coal Runs - Summary of Results

RUN NO	FEED RATE (kg/hr)				(°C)		G.H.V.	G.Y.		GAS ANALYSIS (DRY BASIS)					% C recovered	G.H.V.	G.Y.		INIT. BED WT (kg)	FINAL BED WT (kg)	GAIN / LOSS in BED WT (kg)
	m_c	m_{O_2}	m_s	m_{ch}	$\bar{T}_b$	T_{max}	m³/m³	m³/kg	kg/kg	H_2	CO	CO_2	CH_4	N_2							
101	44.54	25.46	96.66	–	813.8	873	9.09	0.92	0.572	32.43	31.03	32.53	3.74	0.27	35.15	404.87	$0.064 m^3$	2.170	17.97	52.61	34.64
102	27.25	26.91	73.91	–	871.3	894	8.88	0.77	0.988	34.93	22.42	37.26	5.12	0.17	28.43	241.98	$2.83 \times 10^{-3} m^3$	2.712	17.97	48.86	30.89
103	32.49	26.35	72.49	–	897.8	927	9.48	1.52	0.811	36.95	29.77	29.58	3.71	0.00	54.69	308.01	$4.68 \times 10^{-3} m^3$	2.231	17.27	40.91	23.62
104	24.63	26.14	72.37	–	921.8	937	9.03	1.64	1.061	35.29	30.73	30.98	2.76	0.23	60.27	222.44	$6.65 \times 10^{-3} m^3$	2.938	15.91	26.02	10.11
105	24.63	25.36	72.37	–	984.2	1013	9.16	1.79	1.030	36.76	31.95	28.75	2.26	0.30	64.42	228.61	$7.28 \times 10^{-3} m^3$	2.938	16.02	18.98	2.95
109	19.30	25.02	77.93	–	971.8	1027	8.77	2.25	1.297	36.92	28.85	31.76	2.15	0.32	80.76	169.23	$1.17 \times 10^{-2} m^3$	4.038	10.68	14.55	3.87
110	16.14	25.21	72.37	–	917.1	980	9.02	1.645	1.562	39.32	29.03	29.62	1.98	0.06	56.95	145.54	$1.82 \times 10^{-2} m^3$	4.670	13.75	16.02	2.27
111	20.35	24.92	82.67	2.006	924.6	959	8.036	2.27	1.112	34.80	25.45	29.33	1.98	9.44	72.36	163.33	$1.11 \times 10^{-2} m^3$	4.062	13.94	26.14	12.20

RUN 101 - 105 CHAR BED RUN ON BALMER COAL
RUN 109 - 111 CATALYTIC BALMER COAL RUN

* m_c COAL, MAF BASIS; $m_{O_2} = m_{O_2} + .23 m_A$ m_{O_2} = PURE OXYGEN $m_{CA} = m_c + m_{ch}$ m_{ch} = CHAR, MAF BASIS

Table A-4 Ash Agglomeration Trials - Summary of Results

RUN NO	FEED RATE (kg/h)				(°C)		G.N.V.	G.Y.	m_{cv} / m_c	GAS ANALYSIS (DC) BASIS					% C IN ASH	G.N.V. * m_c	G.Y./m_c	m_a/m_c	INIT. BED WT (kg)	FINAL BED WT (kg)	GAIN/LOSS IN BED WT (kg)
	m_c	m_{a_a}	m_a	m_{ca}	$\bar{T}_a$	T_{max}	m³/m²	m³/kg	kg/kg	H_2	CO	CO_2	CH_4	N_2							
97C	29.68	27.18	65.23	–	857.5	996	9.23	1.02	0.916	37.75	30.52	28.72	2.56	0.45	42.41	273.96	3.44×10³	2.198	17.73	5.68	-12.05
98	34.94	27.18	67.23	–	863.8	900	9.14	1.68	0.778	36.76	27.37	32.08	3.65	0.14	71.57	319.35	4.81×10³	1.924	17.64	12.05	-5.59
99	30.99	27.16	71.73	–	884.2	895	8.38	1.83	0.876	38.32	24.47	34.80	2.07	0.33	75.53	259.70	5.91×10³	2.315	16.04	9.89	-6.15
100	33.44	26.10	72.67	–	805.0	818	8.79	1.81	0.781	29.14	22.02	34.95	3.65	0.24	73.95	293.94	5.41×10³	2.173	16.04	10.91	-5.13
107	28.61	29.57	72.42	–	1094	1141	8.71	1.94	1.034	35.16	33.58	29.84	1.06	0.37	71.42	249.19	6.7[illegible]×10³	2.531	13.64	7.27	-6.26
108	30.92	29.92	72.47	–	1039	1017	9.05	1.89	0.968	37.08	33.85	27.50	1.25	0.33	67.57	279.82	6.10×10³	2.344	15.45	28.30	12.84
112	26.93	29.30	68.04	–	1204	1183	8.594	2.21	1.088	36.00	31.60	31.01	1.11	0.29	80.57	231.43	8.22×10³	2.526	14.38	11.25	-3.13

RUN 97C – 100 ASH AGGLOMERATION RUN ON FORESTBURG COAL
RUN 107 – 108, 112 ASH AGGLOMERATION RUN ON BALMER COAL

* m_c COAL HAF BASIS ; $m_{a_a} = m_{a_s} + 23 m_s$ m_{o_2} = PURE OXYGEN $m_{cv} = m_c + m_{ca}$ m_{ca} = CHAR, HAF BASIS

Table A-5 Particle Size and Size Distributions of Coal, Cyclone Products and Knock-Out Drum Dust

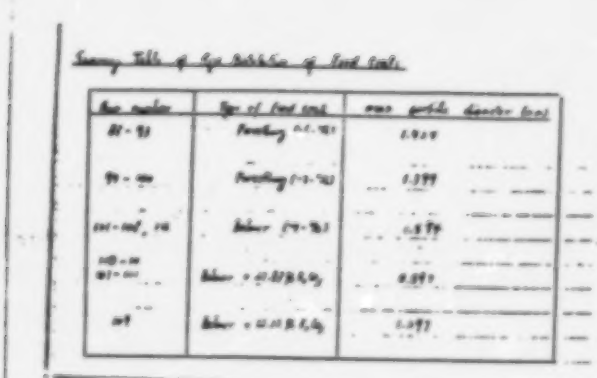

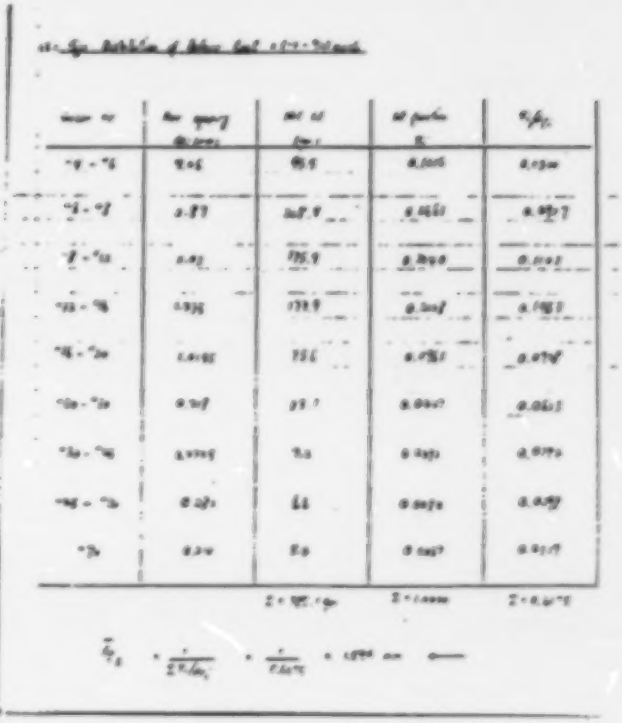

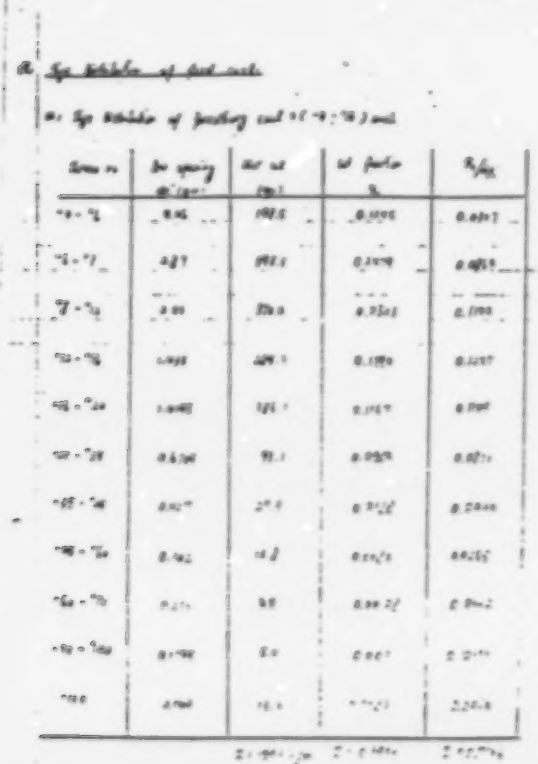

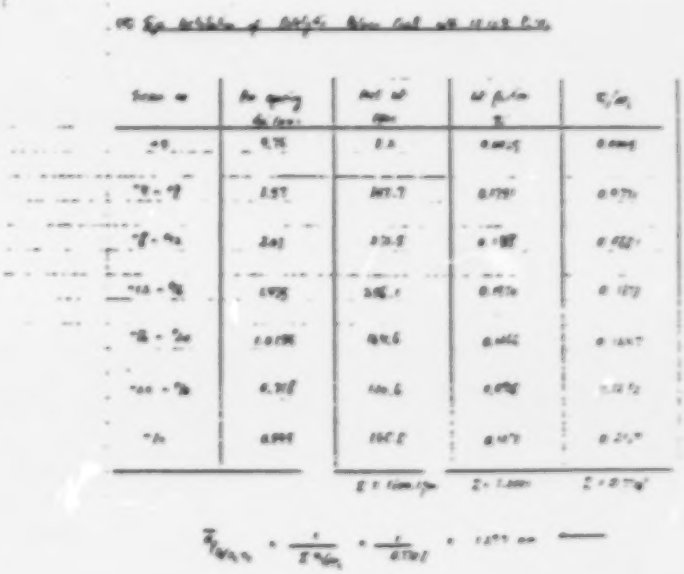

APPENDIX B - EQUIPMENT MODIFICATIONS

During 1983-4 a series of equipment modifications were made to the pilot-plant. In addition to those changes described in the body of the report to permit in-bed sampling, and those discussed as part of the ash agglomeration runs, some other features are new:

(i) All 30 thermocouple readings are now logged on the Doric Digitrend 235 datalogger.

(ii) An overflow drum has been installed (Fig. B-1).

(iii) A baghouse was constructed to replace the existing dust knock-out drums (Fig. B-2, Fig. B-3). This unit gave considerable problems due to plugging of the bags.

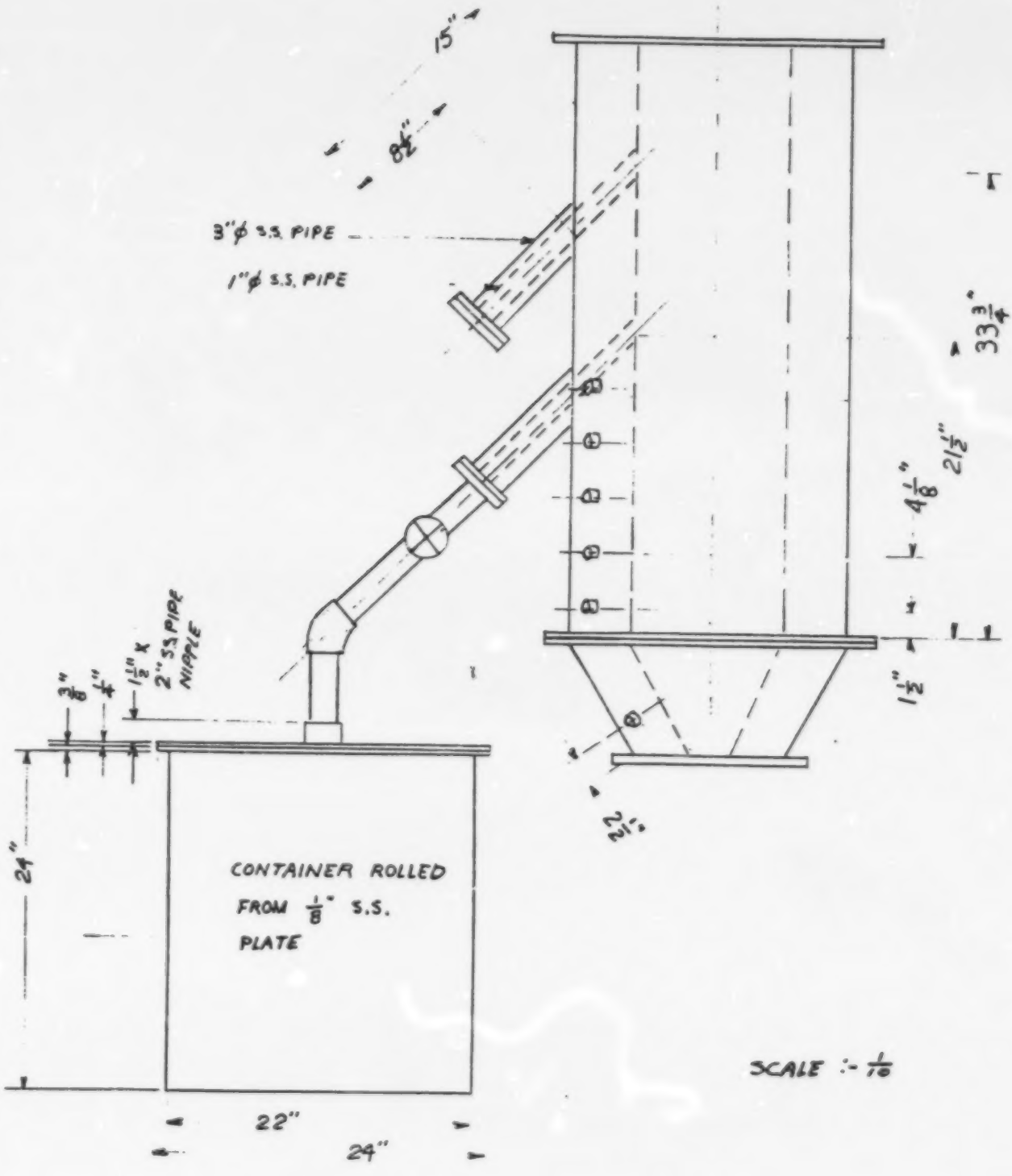

Fig. B-1 6 GAS SAMPLING PORTS AND BED OVERFLOW SYSTEM

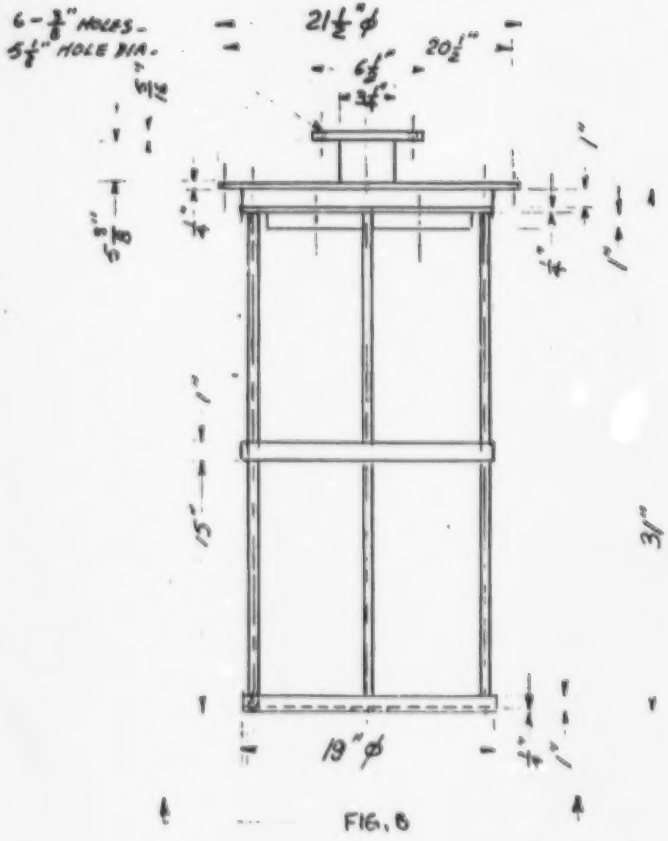

FIG. A :- NOT TO SCALE

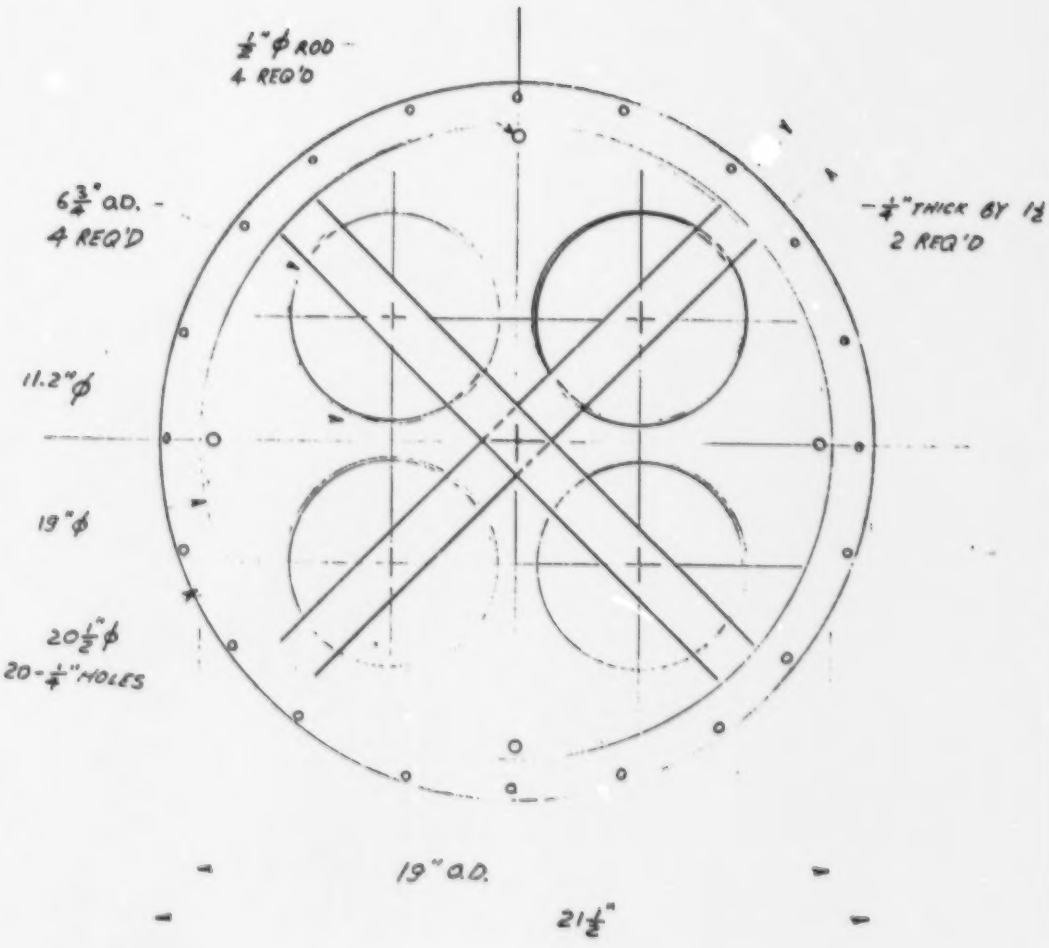

FIG. B :- ¼ SCALE

Fig. B-2 FILTER BAG MANIFOLD

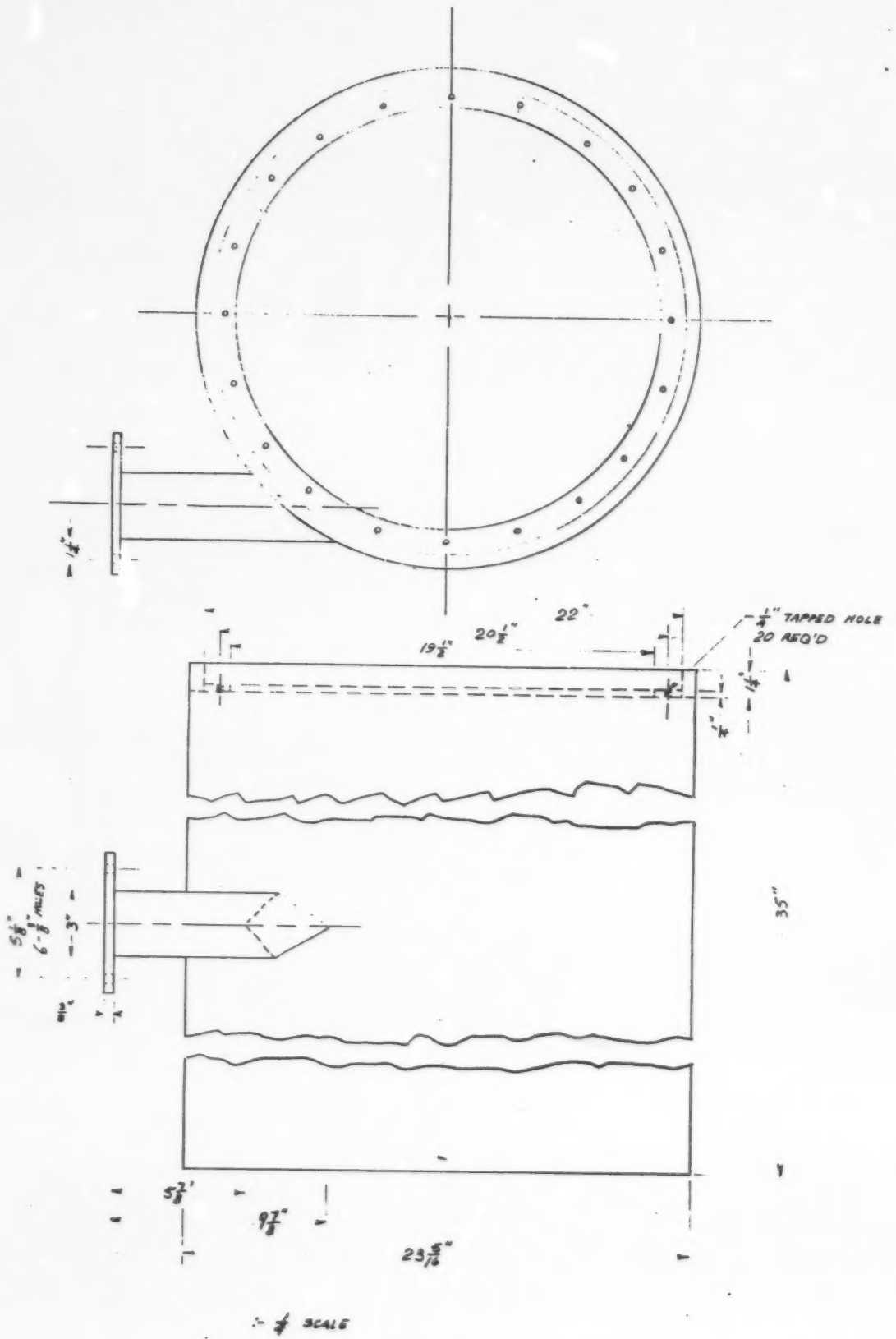

Fig. B-3 FILTER BAG HOUSING

APPENDIX C

Objective:

This project is part of a continuing program for the development of the Spouted Bed as a Gasification Reactor. Specific objectives of the current work program are concerned with an investigation of potential scale-up problems, evaluation of deleterious raw gas constituents, catalytic gasification and reactor modelling. A detailed breakdown of these objectives is as follows;

i) Assesment of reactor stability when operating with char beds of caking and non-caking coals.

ii) Evaluation of the feasibility of char bed operation in a dry ash agglomerating mode accompanied by ash withdrawal. Effect of sorbent additions on ash agglomeration and reactor stability.

iii) Reactor operation with wide sieve size fractions of coal to assess the effect of fine particulates in the coal feed.

iv) Assessment of particulate and sulphur species in the raw gas, in-order to aquire data for the design of removal processes.

v) Preliminary experiments to determine the feasibility of applying catalysts to gasify less reactive bituminous coals. Influence of catalyst additions on reactor stability.

vi) Continuing measurements of gas composition and temperature profiles within the gasifier for the purpose of developing a mathematical model for reactor scale-up.

Task 1 ; Modification of the Reactor.

In order to provide for operation in the ash agglomerating mode, for runs with char beds and for extended runs, modifications to the reactor to provide for ash and char removal are necessary. For char removal by solids overflow, one or two ports (permitting bed height variation) will be added to the top of the reactor. Char removal will be achieved by gravity flow to a sealed vessel via inserts in the shell and refactory linning. The design of these inserts will be similar to existing arrangements adopted for bed sampling. Agglomerated ash will be withdrawn from the bottom section of the bed, near the cone, by density and particle size seggregation in the bed. A modification along the lines of that intended for bed overflow will be necessary. In order to maintain a constant bed height, some means of metering the ash withdrawal rate via a simple feedback control loop will be necessary. To achieve ash agglomeration in the reactor cone, arrangements for oxygen enrichment and steam injection (to control temperature excursions) are necessary. With these modifications, there may be a need to re-line sections of the gasifier refactory linnings.

APPENDIX C - cont'd

Task 2 ; Char Bed Runs with Non-Caking Coals.

The first experimental runs with char beds will be attempted with Forestburg coal. Running conditions will be selected wher possible to correspond to velocities attained in inert beds, at temperatures greater than 850 C. Initial runs will use air and steam as the spouting fluid for optimum air coal ratios and coal feedrates. About 4-5 runs of 6-12 hours duration will be attempted. A typical operating procedure for these runs is described in Appendix B. Two or three extra runs with limestone or dolomite feed will also be attempted to assess th effect on sulphur retention and reactor stability. The sorbent feedrate will be selected to achieve maximum sulphur retention in the bed. The sorbent will be pneumatically conveyed to the reactor via an independent metering device. Additional runs (4-6) to confirm satisfactory operation of char beds (with and without sorbent addition) will be attempted with oxygen and steam as the spouting fluid. For the above runs, coal feeds o narrow and wide size cuts (-4 + 16 and -4 mesh) will be utilised to evaluate the effect of fines, with recycling of fines throughout.

Task 3 ; Char Bed Runs with Caking Coals.

Task 2 will be repeated with a bituminous Balmer or Skunka coal. Again 6-7 runs with variations in coal size distribution, sorbent feed, oxygen and air as the spouting fluid will be attempted.

Task 4 ; Preliminary experiments in the ash agglomerating mode.

Experiments in Tasks 2 and 3 are specifically concerned with reactor stability when operating with predominantly char beds. The ash leaves the gasifier conveyed in the gas. For long periods of operation, this rate of removal may not be satisfactory to prevent ash build-up in the reactor. For experiments in this task, specific attempts will be made to agglomerate the ash in the bottom of the reactor, relyin on density and particle size seggregation for ash seperation and withdrawal. This will require higher temperatures in the cone, and may b achieved by oxygen enrichment at low steam rates. Steam injection may be employed to control ash temperatures with desirable effects in promoting the endothermic steam-carbon reaction. Some trial and error is anticipated to obtain satisfactory agglomeration and removal of ash.

Preliminary experiments may be done in a semi-batch mode, being dependent on the difficulties encountered. Continuous ash removal with caking and non-caking coal feed is the prefered goal of this task.

Task 5 ; Ash Agglomeration with Caking and Non-caking Coals.

Depending on the success achieved in Task 4, a series o 4-6 runs in the ash agglomerating mode will be made for a range of optimum conditions (established in Task 4) with caking and non-caking coals. Sorbent feed will be employed as a parameter.

APPENDIX C - cont'd

Task 6 ; Catalytic Gasification.

A preliminary series of tests with catalytic gasification will be carried out. In 3 or 4 experiments coal will be either pretreated with different levels of potassium carbonate solution, dried and fed to the reactor, or the solution sprayed directly into the cone section of the bed. Short runs will be made to determine the increase in gasification efficiency, change in the gas composition, gas heating value and carbon conversion in the reactor. A simple mass balance will be attempted to determine the distribution of catalyst from an analysis of bed ash and entrained particulates. A less reactive bituminuous coal with a low potassium oxide content in the ash would be prefered for these tests.

Task 7 ; Characterisation of Deleterious Raw Gas Constituents.

Attempts will be made to characterise particulate and sulphur species in the gas leaving the reactor. The task will cover work over several months and will involve an examination cyclone efficiency and characterisation of particulates collected in the cyclone and downstream dust filter. Sample dusts will be sent to the Energy Research Laboratories for size distribution analysis. Sulphurous species in the gas will be monitored throughout. It is anticipated that this task will be attempted in conjunction with the other tasks specified above.

Task 8 ; In-bed Composition and Temperature Profiles.

Internal bed gas composition and temperature profiles will be measured for the purpose of developing a mathematical model of the Spouted Bed Gasifier. The work will be carried out as part of a postgraduate research project.

Modelling of the gasifier will be continued, extending the back-mix model to a two-region model with interactions. Data from past years operation in addition to internal bed data will be incorporated.

Task 9 ; Compilation of monthly, final report and presentation.

Brief monthly progress reports (maximum 3 pages) of the work will be submitted to the CANMET Scientific Authority (in 4 copies) These reports should include

i) Extent of the tasks completed.
ii) Amount of money spent.

The final report (15 copies) will give a detailed description of the work performed during each phase of the project. The following format should be adopted;

i) Title page as per standard CANMET format.
ii) Executive Summary in both official languages.
iii) Introduction;

Statement of ...

POOR

QUALITY

ORIGINAL